Feasibility study of mid-head open-loop pumped hydro storage along Michigan's shoreline

Shen, Xin; Allan, Jon W.; Gaden, Marc; Bricker, Jeremy D.

DOI
10.1016/j.est.2025.119878

Licence
CC BY

Publication date
2025

Document Version
Final published version

Published in
Journal of Energy Storage

Journal of Energy Storage 146 (2026) 119878

Contents lists available at ScienceDirect

Journal of Energy Storage

journal homepage: www.elsevier.com/locate/est

Research Papers

Feasibility study of mid-head open-loop pumped hydro storage along Michigan's shoreline

Xin Shen [a], Jon W. Allan [b], Marc Gaden [b], Jeremy D. Bricker [a,c,*]

[a] Department of Civil and Environmental Engineering, University of Michigan, 2350 Hayward, Ann Arbor, MI, 48109, USA
[b] School for Environment and Sustainability, University of Michigan, 440 Church Street, Ann Arbor, MI, 48109, USA
[c] Faculty of Civil Engineering and Geosciences, Delft University of Technology, Stevinweg 1, 2628CN Delft, the Netherlands

ARTICLE INFO

Keywords:
Pumped hydro Storage
Great Lakes shoreline region
Geographic information system
Site identification
Economic feasibility

ABSTRACT

As the energy system undergoes a growing reliance on renewable energy while the role of conventional thermal power declines, a utility-scale energy storage system of sufficient capacity may help to ensure supply reliability. Pumped Hydro Storage (PHS) technology dominates utility-scale energy storage and, with its unique advantages, is poised to serve as a mature solution for addressing the inherent intermittency and unpredictability of renewable energy. Past research on PHS has given priority to a substantial elevation difference, which has led to an underestimation of its potential. Therefore, this study focuses on mid-head PHS (30–100 m) and explores its technical feasibility in the Great Lakes region, where large natural basins and suitable topography provide favorable conditions for this type of PHS, aligning with the possible future development of lake-based wind power, indicating potential synergies in power integration and infrastructure co-location. This study identifies the distribution of potential open-loop PHS sites along the Great Lakes shoreline within Michigan and demonstrates that their storage potential far exceeds the storage required for carbon reduction goals in the following decades. The economic analysis also demonstrates that the levelized cost of energy (LCOE) for these storage systems, which meet the demand, is only $30–40/MWh, far lower than other utility-scale energy storage technologies. The study also conducts a sensitivity analysis on the technical parameters of site identification, aiming to address various circumstances regarding preferences and conditions, and demonstrates that the storage in each scenario still far exceeds the required amount.

1. Introduction

The International Energy Agency (IEA) projects that renewable energy sources will account for 90 % of global electricity generation by 2050 [1]. As renewable energy continues to grow rapidly within power systems, energy storage technologies have become the key support for maintaining system flexibility, reliability, and energy security [1–5]. Among these, Pumped Hydro Storage (PHS), as the most mature and economically feasible long-duration energy storage technology [6–11], remains the dominant form of utility-scale energy storage worldwide [12]. It is widely recognized as a mature, reliable, and rapidly responsive solution to address the intermittency of wind and solar power generation [13].

Despite the notable advantages that secure PHS a significant share among various energy storage technologies, a substantial elevation difference (water head) [14] has remained a rigid criterion, limiting the applicability of PHS [15], hindering its growth potential [16], and leading to an underestimation of its potential and feasibility. Most existing global assessments and inventories of PHS potential have primarily focused on high-head configurations, typically exceeding 100 m, located in mountainous or hilly regions [17–21]. Consequently, regions with gentle terrain, including much of the U.S. Midwest, have been largely excluded from such analyses, creating a research gap in the understanding of low- and medium-head PHS opportunities. Therefore, this study seeks to address this long-standing constraint by reexamining the technical feasibility and economic viability of medium- (30–100 m) and low-head (2–30 m) PHS systems, thereby expanding the traditional application range of PHS and unlocking its potential in low-relief landscapes that have been previously overlooked [22]. In this context, adopting an open-loop configuration, in which natural lakes or runoff-fed rivers serve as the lower reservoir and only the upper reservoir is artificially constructed, can further alleviate topographical constraints

* Corresponding author.
E-mail addresses: xinsh@umich.edu (X. Shen), allanj@jonallangroup.com (J.W. Allan), mgaden@umich.edu (M. Gaden), jeremydb@umich.edu (J.D. Bricker).

https://doi.org/10.1016/j.est.2025.119878
Received 10 July 2025; Received in revised form 18 November 2025; Accepted 11 December 2025
Available online 30 December 2025

and broaden the scope of feasible applications.

In this regard, the shoreline topography of Lake Michigan is particularly notable, combining moderate elevation differences with a vast natural lower reservoir, making it an ideal testing ground for exploring the PHS potential of gently sloping terrains. The Great Lakes have been largely overlooked in previous national-scale PHS assessments [23] due to assumptions of insufficient topographic relief. This study addresses that gap by reassessing the feasibility of medium- and low-head PHS and emphasizing the distinctive suitability of Michigan's coastal terrain for such development. The existing Ludington Pumped Hydro Storage Plant (the second largest PHS facility in the United States [24]) already demonstrates the technical viability of using Lake Michigan as the lower reservoir for open-loop, medium-head PHS systems. As renewable energy targets tighten, global storage demand is projected to increase nearly tenfold by 2050 [25]. Meeting this demand will require a reconsideration and expansion of PHS siting constraints, underscoring the importance of reassessing regions such as Michigan's Great Lakes shoreline.

This reconsideration is especially relevant given the past and near-future proliferation of wind turbines along and potentially within the lakes. Given the vast potential of lake-based wind power and its spatial compatibility [26,27] with PHS, this co-location of energy generation with large-scale energy storage would allow efficient centralization of power transformation, switching, and transmission. At the same time, the concentration of wind power growth may bring to light the limitations of transmission capacity [28], which can also be effectively mitigated by local energy storage, reducing the excessive wind energy curtailment caused by transmission congestion [29,30]. This spatial and functional complementarity provides essential support for the coordinated development of renewable energy across the Great Lakes region.

In addition, low- and medium-head PHS systems can be designed in ways that reduce ecological disturbance and, given the longstanding public concern and opposition to large-scale energy development in the Great Lakes region [31–34], may provide more practical and socially acceptable alternatives to conventional high-head pumped storage.

Exploring the development of medium-head (30–100 m) pumped hydro storage in the Great Lakes region is both timely and well-suited to the ongoing energy evolution (Appendix A). Therefore, this study aims to explore the technical feasibility of developing medium-head PHS along the Great Lakes shoreline within Michigan by:

1. Conducting a topographical site investigation along the Michigan shoreline (within a certain proximity, after excluding restricted areas) to identify potential sites for PHS development, mapping their near-shore distribution and respective energy storage capacities.
2. Assessing whether the total energy storage potential of these sites can meet Michigan's storage demand in the coming decades. Previous studies have explored a set of methods and criteria for potential site identification, which have been applied to the siting and energy storage potential assessment of rivers, coastlines, and reservoirs [17,35,36]. This study will build upon this methodology, introducing additional considerations for optimization and extending its application to medium-head PHS, additionally examining the spatial overlap between identified sites and high wind energy potential areas to explore opportunities for co-located renewable development.
3. Analyzing the identified sites and assessing whether medium-head PHS as an energy storage technology is economically feasible and competitive at a large scale.
4. Performing sensitivity analysis on the technical parameters of site identification, aiming to address various circumstances regarding preferences and conditions.

The estimated energy storage demand in Michigan for the coming decades is presented in Section 2.1. The methodology for site identification is presented in Section 2.2, followed by feasible energy storage estimation for the identified sites in Section 2.3, and economic analysis in Section 2.4. The results, discussion, and conclusions are provided in Sections 3, 4, and 5, respectively.

2. Methodology

2.1. Energy Storage demand in future Michigan

Midcontinent Independent System Operator (MISO) projects the generation fleet for 2039 based on its historical generation data and operational footprint [37]. MISO developed three future scenarios, varying by their carbon dioxide reduction trajectories. In this study, we focus on the scenario projecting the highest storage demand (Future 3, as presented in their report), as it highlights the upper bound of the critical need to thoroughly investigate energy storage solutions.

Based on MISO's projected storage capacity (GW), we estimate the total annual energy storage demand (GWh) for Michigan in 2039 to be 27,547.97 GWh. Table 2.1 presents the required energy storage assuming daily vs. weekly cycling (charging/discharging) of the PHS infrastructure. These cycling intervals represent typical operational range of PHS systems, providing the lower- and upper-bound estimates of per-cycle storage requirements (calculation details are presented in Appendix B). This table provides a general overview of the energy storage required in Michigan to achieve the future that MISO projects for 2039, which serves as a baseline to evaluate the adequacy of coastal pumped hydro energy storage potential.

2.2. Criteria for site identification

This study focuses on open-loop PHS plants, with the Great Lakes serving as the lower reservoir. Therefore, the site identification process evaluates potential sites for the upper reservoir, focusing on economic feasibility and the absence of geographical restrictions. The specific identification criteria, resembling those applied in previous studies [17,35], will be outlined in the subsequent sections. The topographic analysis for site identification uses a 30-m resolution Digital Elevation Map (DEM) from the United States Geological Survey (USGS) [38], referenced to the North American Datum of 1983 (NAD 1983). Site identification process is conducted in ArcGIS Pro. After potential sites have been identified, the energy storage of each site is calculated based on assumed parameters for pumped hydro storage plants. The calculation is conducted in MATLAB, and the calculation method will be described in subsequent sections.

2.2.1. Search radius and search zone

The search radius defines the inland distance along the Great Lakes shoreline, while the search zone represents the area covered within this radius during the identification of potential upper reservoir sites. These two concepts are referred to as buffer distance and buffer zone in previous studies [17,35]. In the identification process of possible upper reservoirs, the proximity to the shoreline is a significant factor; as the sites move further inland, the length of the penstocks required to connect them increases, making such sites less attractive. The construction cost, maintenance cost, and head loss cost (energy loss due to friction, which result in profit loss) of the penstocks all increase sharply with the increasing length of the penstocks (further discussed in Section 2.4.2.). Therefore, a reasonable "maximum acceptable distance" needs to be set. In this study, this threshold is set at 20 km, an empirical value based on previous studies [17,35,36]. This threshold could, of course, be adjusted in future analyses.

Table 2.1
Minimum and maximum energy storage demand in Michigan.

	Daily Operation	Weekly Operation	Michigan Annually
Energy (GWh)	75.47	528.32	27,547.97

2.2.2. Restricted areas

This study uniquely examines an extensive and intricate shoreline of interest, with the Michigan shoreline serving critical environmental, ecological, historical, and human functions. The development of PHS plants involves numerous complex factors beyond topography and distance from shore, including extensive construction activities, land-use changes, land segmentation caused by long penstocks, ecological impacts, and potential disruptions to local communities. Therefore, understanding the overall shoreline availability is essential prior to conducting site identification. Regions where engineering construction is prohibited or deemed unsafe are categorized as “restricted areas” and excluded in the subsequent site identification process. Restricted Areas are defined using data from various sources, including the Bureau of Land Management (BLM) [39], Michigan Department of Environment, Great Lakes, and Energy (EGLE) [41–45], USGS [46], and Mich. Admin. Code [47]. These areas can be broadly classified into three main categories:

1. Environmental or Ecological Restrictions: Areas designated for protection, such as state parks, national parks and high-risk erosion zones.
2. Land Use Restrictions: Land governed by rights such as common easements or controlled by entities like the Department of Defense.
3. Inland Blocked Restricted Areas: Inland zones rendered unusable due to their adjacency to restricted lakefront areas.

The distribution of restricted areas within the buffer zone along the Michigan shoreline is shown in Fig. 2.1. The corresponding legend is provided in Appendix C.

It should be emphasized that the restricted areas considered in this study are based on preliminary and general expectations. However, this is not definitive; for example, several pumped hydro storage plants (e.g., the Seneca PHS station [48] and Ludington PHS plant [24]) are within the types of restricted areas that were excluded in this study. Furthermore, these expectations are grounded in the current considerations of energy, environmental, and political circumstances, which may evolve as environmental issues intensify, energy demands increase, and energy structures change [49]. These examples are detailed in Appendix C.

2.2.3. Minimum required gross water head

Gross water head is the elevation difference between the water level at the free surface of the lower reservoir (one of the Great Lakes) and the average elevation within the area of each of the identified sites.

The water levels at the free surface of the Great Lakes are approximations based on the average water levels derived from observation data at all stations along the Michigan shoreline. The observation data are sourced from the database of National Oceanic and Atmospheric Administration (NOAA) [50] and are based on the International Great Lakes Datum (IGLD) 1985. Historical data have also been taken into consideration [51]. In this study, the water level of Lake Superior is set at 183.30 m, while the water level of the hydrologically connected Lakes Michigan and Huron is set at 176.60 m.

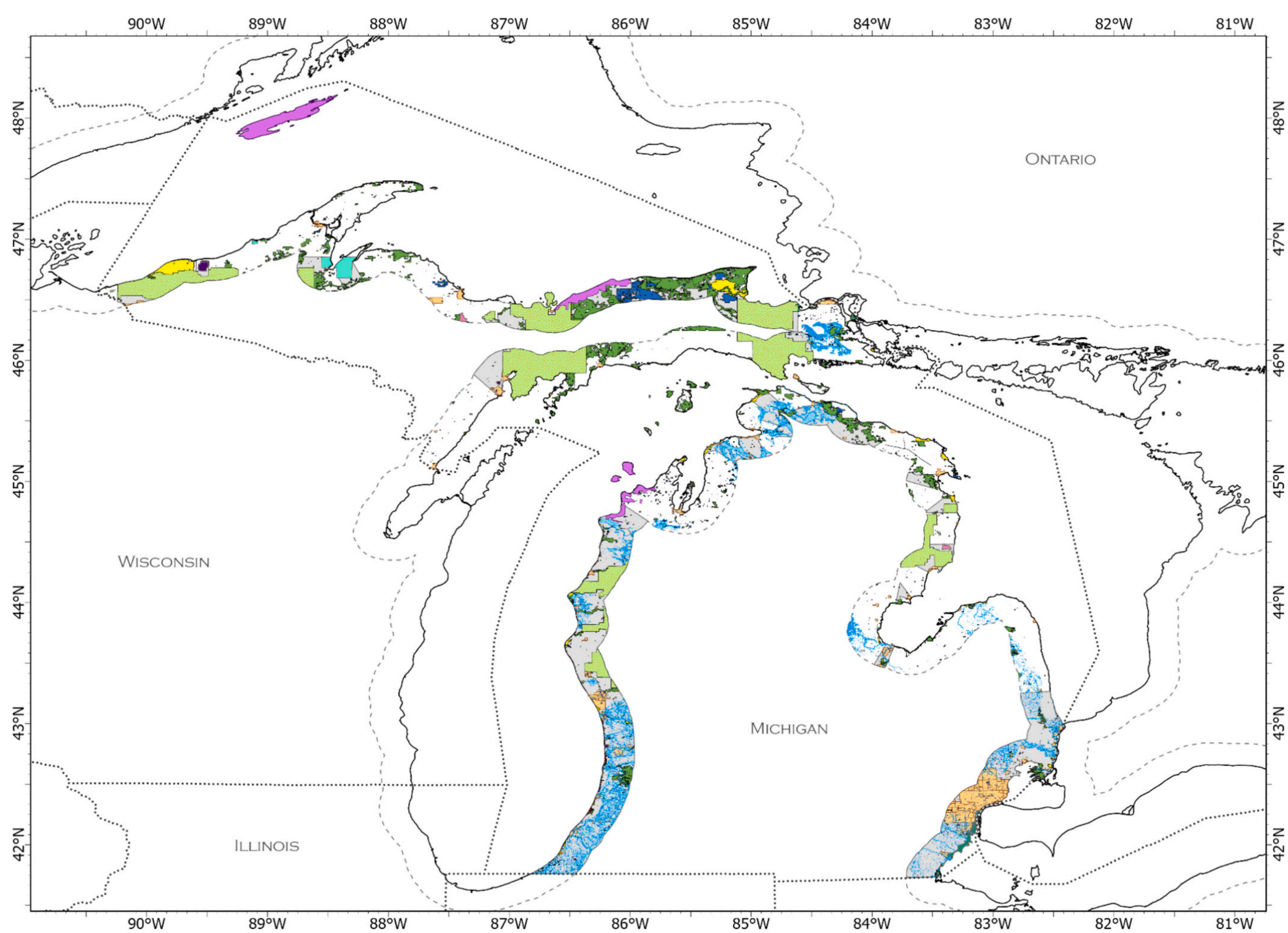

Fig. 2.1. Distribution of restricted areas (colored areas are restricted, with details in Appendix C).

2.2.4. Maximum allowable land slope

The maximum slope serves as the threshold for the 'maximum acceptable slope' within the identified potential sites of the upper reservoir. Only sites with ground slopes ranging from 0 % to this threshold will be retained in the identification process. This criterion is established because a relatively low slope (i.e., flatter area) is preferred to minimize the amount of cut and fill required during civil work for construction of the upper reservoir.

2.2.5. Sensitivity analysis to gross water head and slope

In this study, a sensitivity analysis to both gross water head and slope is included to present the varying scales of pumped hydro storage plants and the different methods to meet the energy storage demand within Michigan. The existence, distribution, and capacity of potential sites are very sensitive to the criteria set in the site identification process. A stricter combination of thresholds (i.e., higher gross water head and lower slope) will filter out more potential sites, and vice versa. Meanwhile, different geographical conditions may suit different demands and circumstances, with no inherent superiority among them. Therefore, a series of gross water heads and acceptable slope values are established, and their combinations will provide various possibilities for discussion under different demands or preferences.

The upper limit for minimum required water head is set at 100 m, based on a comparison with the gross water head of the largest operational pumped hydro storage plant in Michigan, Ludington, which is 110 m [24]. The lower limit for minimum required gross water head is set at 30 m, which is defined as the lower limit of the mid-head range. Fifty meters and 75 m are chosen as well for sensitivity analysis between the two extreme thresholds for minimum required head difference. The middle range of the maximum acceptable ground slope is set at 0 %–5 % based on previous studies [17,35]. As a sensitivity analysis, land slope ranges of 0 %–3 % and 0 %–7 % are also considered. Each scenario for site identification is formed by selecting one of the four options for gross water head, and of the three options for maximum acceptable ground slope. The results of all scenarios are included in Section 3.

2.2.6. Minimum reservoir area

In this study's site identification process, a minimum reservoir area threshold of one acre (≈4047 m^2), is applied to exclude excessively small potential sites that constitute spatial noise from the perspective of economic and practical feasibility. This threshold approximately corresponds to the typical scale of land parcels. Although previous studies have typically selected a 50,000 m^2 threshold [17,52], a lower minimum threshold of upper reservoir area is anticipated here, considering the growing public resistance to large-scale projects in Michigan, particularly when such projects require the utilization of public natural resources [53,54].

2.3. Feasible energy Storage estimation for PHS plants

Pumped hydro storage plants typically consist of an upper reservoir, a lower reservoir, and a power plant that operates dual-functionally: either pumping water to the upper reservoir for energy storage or releasing water to the lower reservoir for energy generation. A schematic representation is provided in Fig. 2.2, and the associated parameters used in the storage estimation are introduced in Appendix D. The calculation of feasible energy storage capacity based on these parameters is presented in Section 2.3, as shown in Eq. 2.2.

With the geometry illustrated in Fig. 2.2, the available storage volume V_{av} of the upper reservoir is approximated as a conical frustum, given in Eq. 2.1. This approximation assumes a balanced cut-and-fill for reservoir excavation and dam raising and incorporates typical engineering allowances such as dead storage and freeboard.

$$V_{av} = \pi/3 \bullet (h_{above} + h_{below}) \cdot \left(R_{top}^2 + R_{bottom}^2 + R_{top} \cdot R_{bottom}\right) \quad (2.1)$$

Building on the available storage volume V_{av} defined in Eq. 2.1, the total theoretical energy storage E_{tot} is obtained as the gravitational potential energy of the water stored in the upper reservoir and is proportional to the product of the available storage volume V_{av} and the available head H_{av} (as shown in Fig. 2.2). Considering friction losses

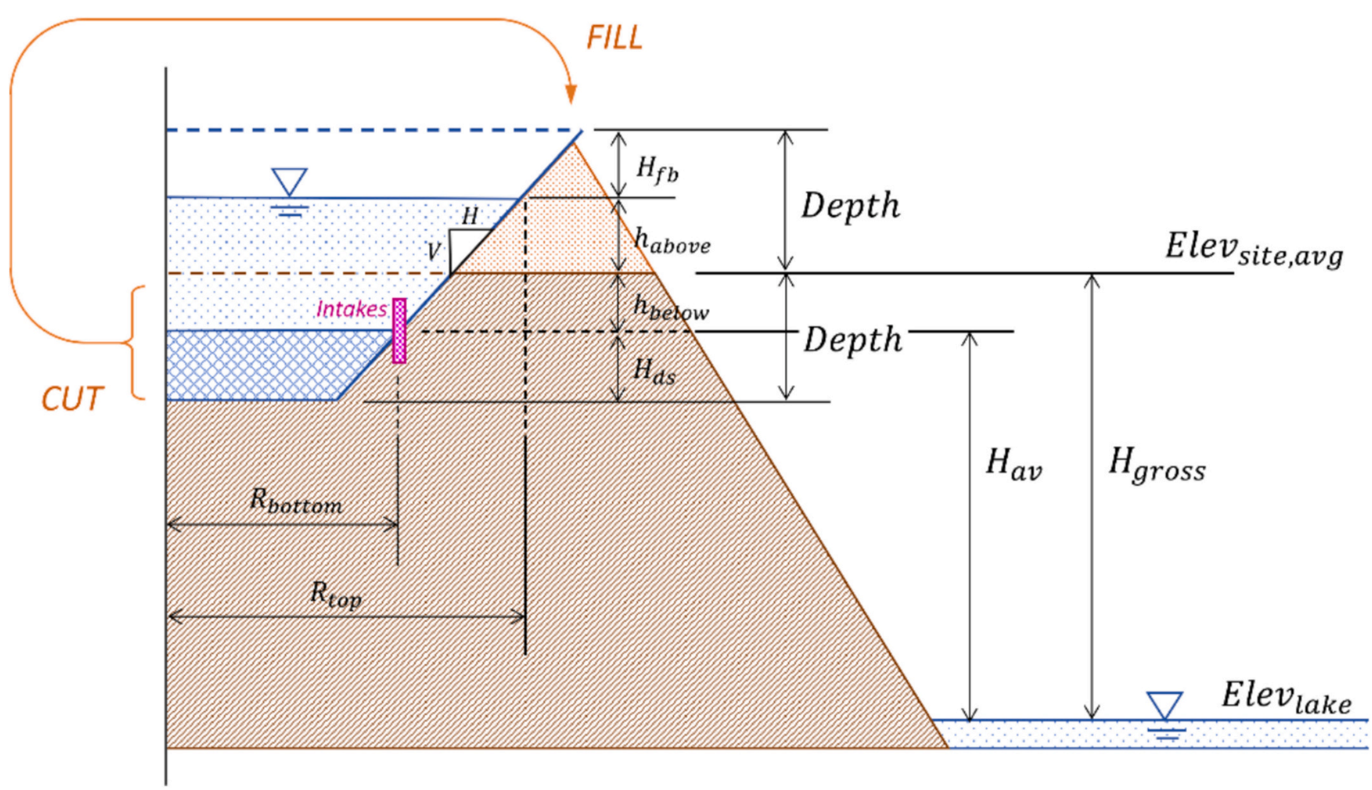

Fig. 2.2. Parameters of PHS plants (Diagram: X. Shen).

along the penstock, the feasible energy storage $E_{feasible}$ is then computed as Eq. 2.2.

$$E_{feasible} = E_{tot} - E_{Loss} \tag{2.2}$$

The parameters and their derivations used in Eq. 2.1, as well as the calculations of E_{tot} and the frictional energy loss E_{Loss} in Eq. 2.2, are provided in Appendix D.

Note that friction losses decrease with increasing penstock diameter; therefore, an optimization process is required to identify a diameter that minimizes such losses. This optimization is introduced in Section 2.4.2.

2.4. Economic analysis

In this study, the economic feasibility of mid-head PHS will be guided and quantitatively assessed from two directions:

Based on the Locational Marginal Price (LMP) pricing model we calculate the potential profits from arbitrage that PHS plants can achieve during charging and discharging, and provide a quantitative profit metric for further relevant research. This is presented in Section 2.4.1.

More importantly, based on the buying period LMP derived from the arbitrage model, another widely used quantitative standard, the Levelized Cost of Energy (LCOE), will be introduced as a methodology. LCOE is a metric that quantifies the average cost per unit of energy stored by an energy storage system over its entire lifecycle. The LCOE for the previously identified potential sites will be provided for analysis and comparison, using the penstock cost obtained from the innovative penstock optimization introduced in Section 2.4.2. This method is presented in Section 2.4.3.

In addition, a preliminary life cycle assessment (LCA) has been conducted to explore potential environmental impacts. This is discussed in Section 2.4.4.

2.4.1. Arbitrage and LMPs during selling and buying periods

LMP is a marginal-cost-based pricing model for the electricity spot market [55], widely used in U.S. power markets [56]. While LMP fluctuates both temporally and spatially, it provides an opportunity for pump-hydro storage plants to profit through arbitrage: buying electricity and pumping water during low-price hours, and generating and selling electricity during high-price hours. The difference between the generation revenue and the pumping cost is defined as the profit. Arbitrage is the primary criterion of the profitability of PHS plants.

Based on previous studies [57–60] and historical Michigan Hub LMP data from MISO [55,61] (April 2024 to August 2024), this study identifies a 6-h selling window with the highest period-averaged LMP and an 8-h buying window with the lowest period-averaged LMP. The start and end times of these windows and their corresponding average LMP values are presented in Table 2.2 (calculation details are presented in Appendix E). Unlike studies that approximate arbitrage using the daily minimum and maximum hourly LMPs [60], this window-based approach reflects the multi-hour cycles observed in real PHS plants.

The period-averaged LMP of the buying window is used as the charging cost in the LCOE calculation (Section 2.4.3). Moreover, based on the principle of energy arbitrage, the profit per cycle is proportional to the price difference between the period-averaged LMPs of the selling and buying windows; thus, a larger difference yields a higher arbitrage profit.

Table 2.2
Hourly average LMP and period-specific averages for selling and buying windows (April–August 2024).

	Buying Period (8 h)	Selling Period (6 h)
Hour of Day	0:00–8:00	15:00–21:00
Period-Averaged LMP ($/MWh)	22.17	45.47

2.4.2. Penstock optimization

The cost of long penstocks and the associated friction loss are significant components of the economic analysis. For large feasible reservoirs multiple penstocks are often required to satisfy the substantial discharge during operation, making the economic assessment of penstock diameter particularly important. However, such optimization is not commonly incorporated into site-level economic assessments.

The penstock diameter is optimized by balancing two opposing effects: larger diameters increase construction and maintenance costs, but reduce friction losses and the resulting energy and revenue losses. The optimization also incorporates practical engineering constraints, including the maximum transportable diameter and the allowable flow velocity range to avoid sediment deposition and scoring. The resulting economic diameter is subsequently used to evaluate frictional energy loss and penstock costs in the LCOE calculation (Section 2.4.3). Detailed calculations are presented in Appendix F.

2.4.3. Levelized cost of Storage and Levelized cost of energy

Levelized Cost of Energy (LCOE) is a widely used metric that represents the discounted average cost per unit of energy over the entire lifecycle of an energy system [62–64]. In this study, LCOE includes capital expenditures and annual operation and maintenance costs, within which the charging cost is incorporated. The charging cost is based on the buying-period averaged LMP from Table 2.2 and functions analogously to the fuel cost in LCOE calculations for energy generation technologies (parameters and detailed calculations are presented in Appendix G).

In this study, LCOE is selected as the metric for economic analysis because it offers insight into the energy price necessary to achieve a net present value (NPV) of zero (i.e., cost recovery), enabling direct comparison with real-time LMP on the power market [65]. Moreover, it provides a standardized framework for evaluating different energy storage technologies, thereby facilitating the following comparison with LCOE assessments in other studies.

2.4.4. Life cycle assessment

Life Cycle Assessment (LCA) is an internationally applied environmental assessment method used to examine the impacts of pumped hydro storage (PHS) facilities from a full life-cycle perspective, covering construction, operation, and decommissioning. However, the storage plants assessed in this study remain conceptual, and their environmental impact outcomes would depend substantially on factors such as site location, operational lifetime [66], and the energy sources used for charging [67]. Therefore, no quantitative environmental impact indicators are provided in this stage of the analysis. Nevertheless, this study refers to sustainability indicators commonly used in the literature, including the Energy Stored on Invested (ESOI) [8] and Global Warming Potential (GWP) [66,68–70], to conduct a qualitative assessment of the long-term environmental performance of PHS, and, drawing on existing research and relevant engineering practice, to discuss potential long-term environmental impacts. Further details are provided in Section 4.3.

3. Results

Under each combination of water head and acceptable slope criteria established in Section 2.2.5, potential sites for the upper reservoir are identified and evaluated. Section 3.1 presents the energy storage capacity of all potential sites in Michigan as a whole, Section 3.2 presents the site distribution, and Section 3.3 presents the economic evaluation of the potential sites based on LCOE. Consistent with Section 2.2.2, sites within restricted areas have been excluded from the analysis. Accordingly, all reported results and site distributions reflect only the feasible potential sites identified outside the restricted areas.

3.1. Energy Storage estimates by siting criteria

Table 3.1 presents the total energy storage of all potential sites within Michigan under each combination of gross water head and acceptable slope criteria, excluding sites within restricted areas.

3.2. Distribution of potential sites

In order to maintain brevity, the site distribution maps only present two extreme scenarios: 100 m minimum water head with a 3 % maximum acceptable ground slope, and 30 m minimum water head with a 7 % maximum acceptable ground slope. These represent the most and least stringent siting criteria, respectively, resulting in the smallest and largest number of potential sites, as well as the lowest and highest total energy storage. For clarity, these two scenarios are hereafter referred to as the least storage scenario (LSS) and the greatest storage scenario (GSS), respectively. Fig. 3.1(A) illustrates the LSS, characterized by a 100 m minimum water head and a 3 % maximum acceptable ground slope, while Fig. 3.1(B) illustrates the GSS, characterized by a 30 m minimum water head and a 7 % maximum acceptable ground slope. The figures are presented in the form of a categorized scale chart:

1) Each dot on the map represents a potential site, and its spatial pattern reflects the geographic distribution of potential sites. It is evident that all dots fall within the 20 km shoreline search zone and avoid the restricted areas depicted in Section 2.2.2.
2) The energy storage of each potential site is represented by both the color and size of the dots. The color broadly indicates the scale of energy storage (GWh) for each site, while the size of the dot provides a visual comparison of the storage magnitude across the various potential sites.
3) The potential sites do not overlap geographically, even though they may appear to do so on the map. This apparent overlap is due to the close proximity of certain sites and the use of scaled symbols, which may lead to partial occlusion in densely clustered areas.

It should be noted that the combinations of gross water head and acceptable slope criteria are not linearly hierarchical, meaning that different head–slope pairs do not necessarily yield nested sets of potential sites. As a result, certain sites identified under the LSS do not appear in the GSS. The detailed dataset of potential site locations and their corresponding attributes will be made openly available through the Deep Blue Data repository, as described in the Data Availability Statement.

3.3. Levelized cost of energy

Similar to the site identification process and the distribution maps presented in Fig. 3.1, Fig. 3.2 and Fig. 3.3 illustrate the LCOE of all potential sites under the same two extreme scenarios: Fig. 3.2 corresponds to the least storage scenario (LSS), characterized by a 100 m minimum water head and a 3 % maximum acceptable ground slope, while Fig. 3.3 corresponds to the greatest storage scenario (GSS), characterized a 30 m minimum water head and a 7 % maximum acceptable ground slope. Each figure consists of two components: a log-histogram, where the x-axis shows the LCOE range (bins) and the y-axis shows the total energy storage (on a logarithmic scale) of the potential sites whose LCOE fall within each corresponding bin, and a pie chart that shows the share of energy storage for each LCOE bin.

Table 3.1
Total energy storage per cycle of potential sites in Michigan by gross water head and acceptable slope criteria.

Energy Storage per Cycle (GWh)		Gross Water Head			
		30 m	50 m	75 m	100 m
Acceptable Slope	0–3 %	20,799.70	17,818.60	13,529.30	11,260.41
	0–5 %	34,778.23	32,607.63	27,143.60	23,775.84
	0–7 %	45,394.42	43,588.95	38,658.95	34,658.84

4. Discussion

4.1. Energy Storage and site distribution

The PHS potential within Michigan (Table 3.1**)** substantially exceeds the in-state energy storage demand projected by MISO (Table 2.1), across all combinations of siting criteria, even under the least storage scenario (LSS), characterized by a minimum 100 m water head and a maximum 3 % acceptable ground slope. This flexibility in selecting PHS plants under varying preferences and conditions instills confidence in the development of PHS within the state.

Additionally, it is noteworthy that the majority of potential sites are concentrated in the northwest region of the Upper Peninsula. This distribution does not fully align with the battery expansion projected by MISO [37], nor with the current primary load-demand regions, which are predominantly located in the southern part of the Lower Peninsula (e.g., Detroit and Lansing) [71].

Despite this misalignment with the load-demand regions, the proximity of these potential sites to the vast lake-based wind resources [26,27] enables open-loop PHS systems to operate synergistically with wind generation compatibility. By storing and releasing energy locally on the supply side, intermittent wind power can be converted into dispatchable electricity before transmission, alleviating the need for extensive long-distance, high-capacity transmission lines.

Fig. 3.1 (see Section 3.1) illustrates the distribution of potential PHS sites and the Michigan 50 m (above surface) wind resource. Fig. 3.1(A) represents the Least Storage Scenario (LSS), characterized by a 100 m minimum water head and a 3 % maximum acceptable ground slope, while Fig. 3.1(B) represents the Greatest Storage Scenario (GSS), characterized by a 30 m minimum water head and a 7 % maximum acceptable ground slope.

The wind resource map is provided by the National Renewable Energy Laboratory (NREL) and represents offshore wind resources within a 20 km search radius at a height of 50 m [27,72]. The original NREL wind power classifications have been aggregated, with classes 6–7 merged as "prime resource," suitable for large-scale wind power development; class 5 defined as "moderate resource"; and classes 1–4 aggregated as "limited resource," suitable primarily for small- to medium-scale projects.

Both scenarios reveal a strong spatial concentration of potential PHS sites and "prime resource" wind areas near the Keweenaw Peninsula in the northwest of the Upper Peninsula and around Grand Traverse Bay in the northwestern Lower Peninsula. This spatial overlap indicates a strong co-location potential between potential PHS sites and high-quality wind resources, suggesting highly favorable conditions for the integrated development of wind generation and open-loop PHS in these regions.

This spatial compatibility is of increasing importance and practical relevance given the ongoing energy transition and the past and near-future proliferation of wind turbines along and potentially within the Great Lakes [73]. The co-location of open-loop PHS plants with large-scale lake-based wind power generation can mitigate excessive wind energy curtailment caused by transmission congestion [29,30], as the concentration of wind power growth has revealed the limitations of existing transmission capacity [28]. Moreover, such co-location allows for the efficient centralization of power transformation and switching facilities through shared infrastructure such as high-voltage substations, thereby reducing the need for long-distance, high-capacity transmission lines and enhancing the efficiency of grid infrastructure utilization, reducing integration costs and operational complexity, and in turn strengthening the system-level attractiveness of lake-based wind development [74,75].

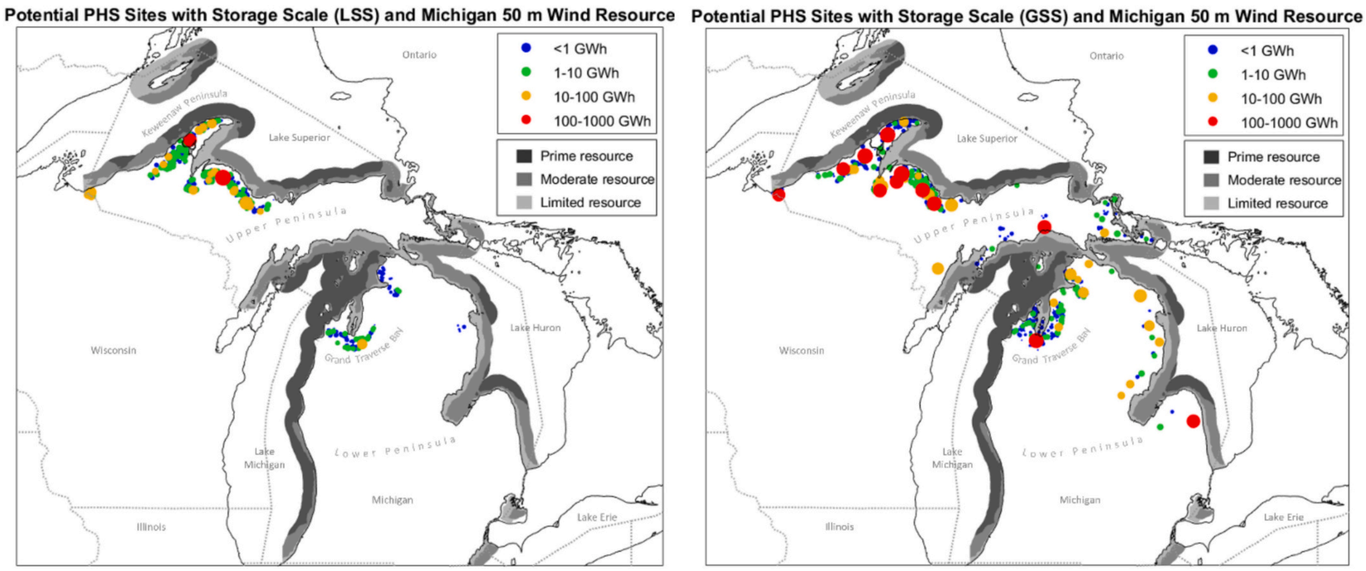

Fig. 3.1. (A) Site distribution under the Least Storage Scenario (LSS) with 100 m minimum water head and 3 % maximum acceptable ground slope, excluding restricted sites, and Michigan offshore wind resources within 20 km of the shoreline at 50 m height.
Fig. 3.1(B) Site distribution under the Greatest Storage Scenario (GSS) with 30 m minimum water head and 7 % maximum acceptable ground slope, excluding restricted sites, and Michigan offshore wind resources within 20 km of the shoreline at 50 m height.

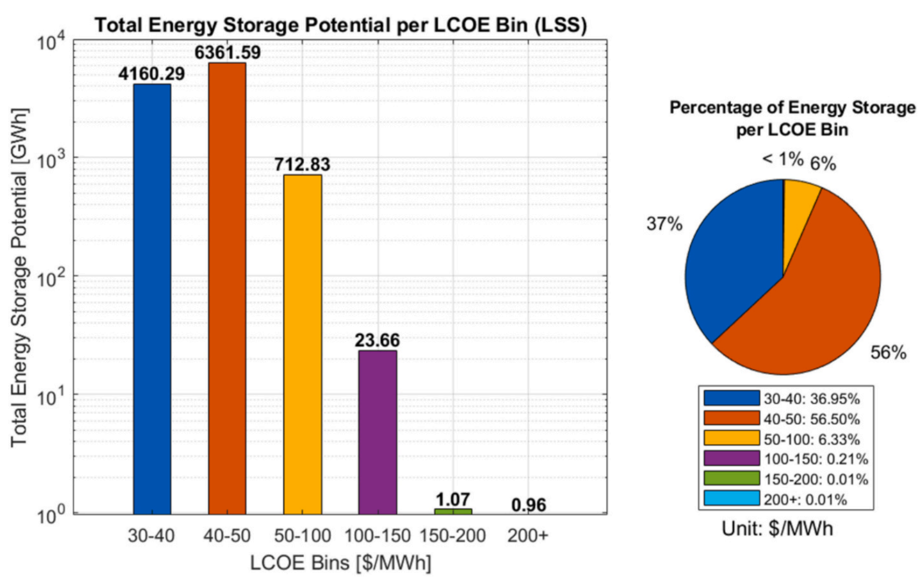

Fig. 3.2. LCOE of the Least Storage Scenario (LSS) with 100 m minimum water head and 3 % maximum acceptable ground slope, excluding restricted sites.

The spatial distribution of potential PHS sites also aligns with regional market signals indicative of heightened flexibility requirements, particularly in the northeastern Upper Peninsula, where high locational marginal prices (LMP), sharp LMP separation, and occurrences of negative pricing are observed. This pattern is widespread across the MISO North region (covering northern Michigan, Minnesota, Wisconsin, and North Dakota) and primarily results from the spatial and temporal imbalance between generation and load [76]. The study shows that transmission congestion, mainly due to line capacity, is not the sole factor behind this market imbalance, and its isolated impact is relatively limited [76]. Repeated transmission expansion efforts have failed to substantially alleviate problems such as wind power curtailment and negative pricing caused by regional congestion [77]. In essence, constructing new long-distance and high-capacity transmission lines solely to address short-lived and regionally confined periods of high prices or price separation often results in low utilization rates, long investment payback periods, and limited economic returns.

Therefore, deploying energy storage facilities such as PHS in these regions represents a more targeted and complementary alternative. Such facilities can locally mitigate generation surplus, alleviate regional price volatility, and at the same time reduce system-level expansion needs [74].

Beyond maintaining generation-load balance and stabilizing electricity prices, PHS can provide a variety of ancillary services that are essential to power system operation [78]. Through inertial response and primary frequency control, PHS helps regulate and stabilize grid frequency, thereby ensuring system reliability by preventing generator trips and cascading outages caused by frequency deviations. In addition, PHS can provide voltage support by regulating reactive power during both pumping and generation modes. It is also capable of providing black-start capability by acting as a self-starting power source during outages, whereas most generators require external power for startup.

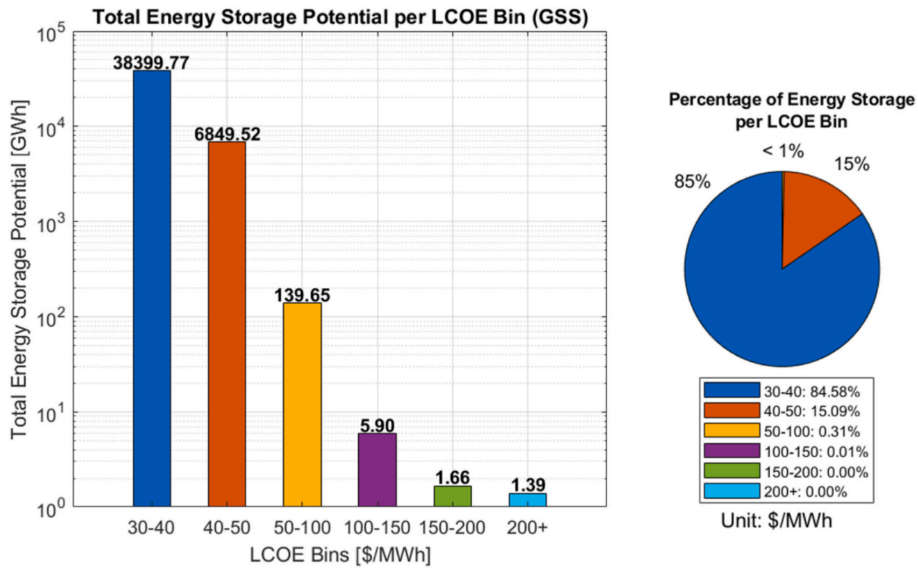

Fig. 3.3. LCOE of the Greatest Storage Scenario (GSS) with 30 m minimum water head and 7 % maximum acceptable ground slope, excluding restricted sites.

This function has become increasingly critical amid the rising frequency and scale of outage events driven by climate change [2,3].

4.2. *Economic feasibility of PHS in Michigan*

The economic feasibility of the identified PHS sites is demonstrated by the fact that the lowest-cost options alone are sufficient to meet Michigan's projected storage demand. As shown in both extreme scenarios (Fig. 3.2 and Fig. 3.3) and the intermediate cases between them, energy storage with an LCOE in the range of $30–40/MWh meets the projected storage demand for Michigan in the coming decades (Table 2.1). In the greatest storage scenario (GSS) (Fig. 3.3), energy storage with an LCOE within the $30–40/MWh range accounts for the vast majority (over 84 %) of the total, while in the least storage scenario (LSS) (Fig. 3.2), although the share of storage with an LCOE in the $40–50/MWh range is greater, the demand is already met by the $30–40/MWh range. As such, the higher LCOE sites are unlikely to be developed.

The difference in LCOE distribution between the two scenarios mainly arises from the distinct sets of identified potential sites, their topographic characteristics, and scale effects. In each scenario, variations in elevation, slope, and distance from the shoreline influence the required engineering works, such as cut and fill volumes and the length of penstocks connecting the upper reservoir to the lower (lake) reservoir. These differences in construction requirements directly affect the overall project cost and, consequently, the resulting LCOE distribution. In the GSS, the effect of scale is particularly evident: more permissive siting conditions allow a larger number of feasible sites, which increases the total capacity and thereby reduces the unit cost. In contrast, in the LSS, stricter siting constraints limit the number of available sites and weaken economies of scale, leading to a higher share of projects with greater LCOE values.

Overall, these findings demonstrate how geographic conditions, engineering requirements, and storage scale collectively shape the cost distribution of potential PHS development in Michigan.

This cost advantage is further supported through comparison with other storage technologies, as illustrated in Fig. 4.2.

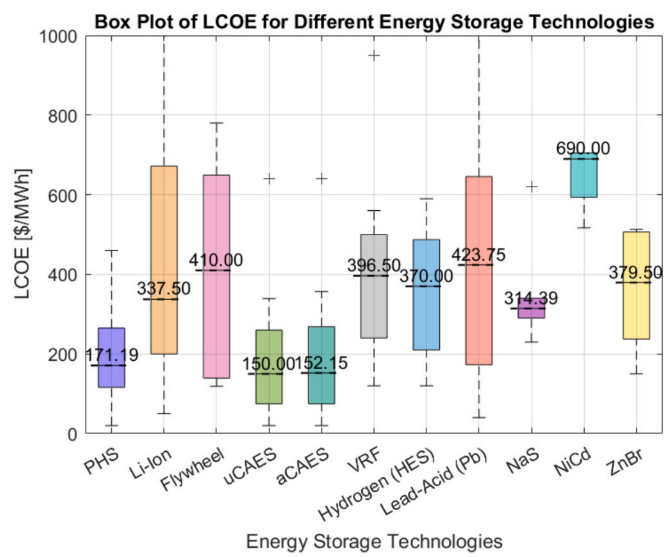

Fig. 4.2. LCOE for different energy storage technologies.

Fig. 4.2 shows a comparison of the LCOE for different energy storage technologies, both current and forecasted, based on multiple studies [79–82,113].

The LCOE of PHS is among the lowest within the storage technologies, and the mid-head PHS in Michigan, as derived in this study, is furthermore positioned at the lower end of the PHS range. This is primarily due to the cost benefits [25] resulting from large-scale capacity and frequent operational cycles. Additionally, this cost also meets the DOE's cost requirements for inter-day Long Duration Energy Storage (LDES) [83].

It should be noted that although the detailed LMP analysis in this study focused on data from April to August 2024, the hourly LMP data for the entire year at the MISO Michigan Hub [61] indicate that the minimum LMP values (corresponding to the charging cost in the LCOE calculation) remained relatively steady throughout most of the year except in December and January. This suggests that the LCOE estimation presented in this study is reasonable and representative. However, the difference between the maximum and minimum hourly LMP values was noticeably larger during the summer months, indicating that the arbitrage potential of PHS is higher in summer.

4.3. Life cycle assessment of PHS in Michigan

In this section, the life-cycle performance of PHS is first evaluated from an energy-efficiency perspective using the Energy Storage on Investment (ESOI). As a direct indicator of sustainability, the ESOI is defined as the ratio of the total energy stored over the lifetime of a storage system to the energy required for its construction. From an ESOI perspective, the development of energy storage systems should give priority to manufacturing durable and long-lasting storage devices while extending their cycle life. A lower frequency of decommissioning, recycling, and reconstruction translates into reduced energy and material requirements to maintain system capacity. According to the study by Barnhart and Benson [8], among all metal-based batteries, the highest ESOI is 32 for Li-ion, whereas PHS has an ESOI exceeding 700, highlighting its superior long-term energy efficiency.

Beyond energy efficiency, the environmental impacts of PHS can also be evaluated through indicators such as Global Warming Potential (GWP). Studies have suggested that the Global Warming Potential (GWP) primarily originates from the construction and manufacturing stage of PHS plants [68,69]. For PHS plant types with reduced construction, this impact decreases [68]. In the present study, the use of the Great Lakes as the lower reservoir reduces the overall civil engineering workload, which can be expected to result in a lower GWP compared to conventional PHS plants.

This environmental advantage is further highlighted in cross-technology comparisons. When comparing utility-scale PHS with various metal-based battery technologies, PHS demonstrates lower impact indicators, including GWP, than all other technologies [66,70]. This is primarily because the lifetime of PHS is much longer than that of Li-Ion batteries, the other popular form of energy storage. Moreover, this difference further increases with the extension of the plant's operational lifetime [66].

While indicators such as ESOI and GWP provide a quantitative basis for comparing the energy and carbon performance of storage technologies, they do not fully capture the long-term ecological implications of PHS. Over the extended lifetime of a PHS facility, which often exceeds several decades, its interaction with local hydrology, aquatic ecosystems, and land use may lead to both direct and indirect environmental impacts.

The construction of PHS facilities may result in significant alterations to land use, such as the development of an upper reservoir, penstocks, and other associated infrastructure. These changes often lead to habitat loss, fragmentation, and degradation. During operation, PHS systems may also interfere with natural flow regimes to varying degrees. The combined effects of construction and operation can alter habitat structures and disturb the behavioral patterns of wildlife, including foraging, reproduction, and migration, thereby affecting the stability of local ecosystems and biodiversity [84]. In addition, PHS projects may exacerbate soil erosion and land degradation [85], and in some cases, are associated with deforestation, soil erosion, and landslide hazards [84].

The construction and operation of PHS facilities may also influence both the quantity and quality of water resources in the Great Lakes region. Operational processes may cause evaporative losses and alter water chemistry, including changes in the concentrations of dissolved oxygen, total dissolved solids, nutrients, and heavy metals, while frequent pumping and discharging cycles can induce shoreline erosion and sedimentation [84,85]. These changes may degrade aquatic habitats and affect environmental as well as socio-economic water uses [85].

For Michigan, the potential impacts of PHS on fisheries require particular attention, as fisheries are not only a key economic pillar of the state but also a vital part of its cultural and regional identity. The impacts on fisheries may be relatively direct and quantifiable, such as the mortality rate of fish larvae in nearshore shallow waters during pumping operations, or the rate of adult fish entanglement in barrier nets, which in turn translate into economic losses for fisheries. However, the potential impacts on related ecosystems, resulting from changes in specific fish species and their ecological niches, are more difficult to quantify. For instance, it remains unclear whether a decline in certain fish species would affect organisms that rely on them (i.e., food web dynamics), or conversely, promote the proliferation of competing or opportunistic species.

These environmental impacts are not static but rather represent a continuous, cumulative, and dynamically evolving process that extends throughout the construction and operation phases of PHS facilities. Although some disturbances may have lasting effects, appropriate mitigation and compensation measures, such as ecological management mechanisms exemplified by the Great Lakes Fishery Trust (GLFT) [86] established for the Ludington project, can partially offset or remediate these long-term impacts.

In the social context, although there might be a general reluctance among the public and local communities in Michigan toward large-scale projects and the commercial utilization of Great Lakes resources [31], partly due to the controversy surrounding the Ludington project [32–34], PHS development and operation can in fact bring broad social and economic benefits, such as creating employment and recreation opportunities, increasing local tax revenues, and enhancing regional energy security [84,87]. While such projects may also cause certain disruptions to local communities, inclusive public engagement and negotiation mechanisms can enable fairer compensation and benefit-sharing, as exemplified by the GLFT [86] mechanism established for the Ludington project. Such mechanisms offer valuable lessons for developing inclusive and equitable local engagement strategies in future PHS projects. Building on these insights, future research may further examine the social acceptance and public engagement dimensions of PHS development.

5. Conclusions

This study reveals that the storage potential of sites located within 20 km of Michigan's shoreline surpasses the projected storage demand estimated by MISO by several orders of magnitude. Furthermore, these sites offer the flexibility to accommodate PHS plants across a wide range of storage scales (in GWh), which underscores the feasibility and adaptability of PHS development across the state. The considerable economies of scale and cost advantages associated with the identified sites underscore their suitability for utility-scale energy storage applications.

In addition, the identified potential PHS sites show a significant spatial overlap not only with areas of high wind energy potential but also with regions characterized by frequent wind curtailment and pronounced price separation. This spatial synergy highlights the opportunity for co-locating PHS and wind generation to enhance grid flexibility and promote integrated renewable energy development across the Great Lakes region.

Building upon these findings, the present study advances the understanding of PHS development by challenging the traditional high-head assumption that has long constrained global assessments of site feasibility. By reexamining the technical and economic potential of medium- and low-head systems, it demonstrates that Michigan's Great Lakes shoreline, once overlooked due to presumed topographic limitations, offers uniquely favorable conditions for open-loop PHS. The analysis also provides new spatial insights into the compatibility of PHS with regional renewable energy expansion. Collectively, these findings not only expand the conceptual and geographic boundaries of PHS site selection but also provide new perspectives for system-level energy storage planning in regions with high renewable penetration.

While these results establish a strong technical and economic foundation, broader social and environmental implications also warrant attention in future planning, particularly given the controversy and public caution historically associated with the Ludington [32–34] project and other large-scale renewable developments related to the Great Lakes [31]. Future studies should integrate social and governance perspectives into the planning process, emphasizing transparent communication and community-specific engagement, and improving mechanisms for dialogue, compensation, and benefit-sharing to ensure equitable and sustainable PHS development in Michigan. In parallel, future work should incorporate ecological modeling and environmental risk assessment approaches (such as hydrodynamic simulations and fish population models) to quantitatively evaluate the long-term impacts of PHS operation on fisheries and aquatic ecosystems. Interdisciplinary collaboration among ecology, fisheries science, and policy governance is also essential to integrate environmental constraints into site selection and project planning frameworks.

Furthermore, evolving environmental and energy circumstances may gradually relax current siting restrictions. For example, the U.S. Nuclear Regulatory Commission is reviewing a proposal (2023) to restart the Palisades Nuclear Plant in Covert, Michigan [88], located within high-risk erosion zones excluded in this study. The case illustrates that previously restricted areas, once proven stable and safeguarded, may remain viable for future energy development.

Beyond the scope of this study, and worth exploring, are broader technological pathways that could open additional opportunities for PHS deployment in Michigan. One direction involves the adoption of more fish-friendly pump–turbine systems [89]. Another promising pathway involves other types of PHS which could be effective in Michigan, such as Pumped Underground Storage Hydro (PUSH), or the repurposing of decommissioned mines for pumped storage. In the Upper Peninsula, particularly in the Keweenaw Peninsula and Marquette Range, where most of the sites identified in this study are located, there are abandoned copper and iron mines, offering potential for exploration and revitalization [90]. Roman Sidortsov et al. (2021) assessed the feasibility of a case study in Negaunee, Michigan [91]. To date, no such projects have been completed in the United States, but it holds promise due to reduced impacts on land use and fisheries, along with socioeconomic benefits that can come with revitalizing abandoned mining sites.

Glossary

ArcGIS Pro A professional desktop geographic information system (GIS) software developed by Esri, used for spatial analysis and mapping.

BLM Bureau of Land Management; a U.S. federal agency that manages public lands and provides geospatial data.

Curtailment The reduction or restriction of electricity generation from renewable sources (e.g., wind or solar) due to oversupply, transmission constraints, or lack of storage capacity.

DEM Digital Elevation Model; a gridded representation of ground surface topography used in spatial analysis.

DOE United States Department of Energy; the U.S. federal agency responsible for energy policy, research, and infrastructure, including long-duration storage planning.

EGLE Michigan Department of Environment, Great Lakes, and Energy; the state agency responsible for managing Michigan's natural resources and environmental data.

Energy Storage capacity The maximum power (in GW) that a storage system can deliver or absorb at any given moment. It reflects the system's instantaneous output or input capability.

Energy storage demand The estimated amount of storage energy (in GWh) required to meet projected grid needs, such as flexibility, reliability, or decarbonization targets.

Energy storage potential The total amount of energy (in GWh) that can be feasibly stored and discharged from a system or site, based on geographic, technical, and design constraints.

ESOI Energy Stored on Invested; a metric representing the ratio of energy delivered over a system's lifetime to the energy required for its construction and operation.

Friction loss The hydraulic energy loss caused by friction between flowing water and the internal surface of the penstock or conduit, typically calculated using the Darcy–Weisbach equation in pumped hydro systems.

GIS Geographic Information System; a digital tool used for spatial analysis and mapping to identify feasible locations for infrastructure.

GLFT Great Lakes Fishery Trust, an environmental trust established in 1996 as part of the Ludington Pumped Storage Project settlement to restore and enhance Great Lakes fishery resources.

IEA International Energy Agency; an intergovernmental organization that provides policy advice, data, and analysis on global energy systems, based in Paris.

IGLD International Great Lakes Datum; a standardized vertical reference system used for measuring water levels in the Great Lakes region.

IHA International Hydropower Association; a global nonprofit organization that promotes sustainable hydropower and provides data, guidelines, and policy recommendations for hydropower development.

LCA Life Cycle Assessment; a systematic analysis of the environmental impacts associated with all stages of a product's or system's life.

LCOE Levelized Cost of Energy; the average cost per unit of electricity generated over the lifetime of an energy system, incorporating capital, operation, and maintenance costs.

LCOS Levelized Cost of Storage; the average cost per unit of energy stored and discharged by a system over its lifetime.

LMP Locational Marginal Price; the cost of supplying the next unit of electricity at a specific location, reflecting generation costs, transmission congestion, and power losses.

LRZ Local Resource Zone; a subregional planning and operational unit defined by MISO to assess transmission capacity, generation resources, and reliability needs. Michigan is primarily located in LRZ 2 (Upper Peninsula) and LRZ 7 (Lower Peninsula).

Mid-head PHS Pumped hydro storage systems with a medium elevation difference between upper and lower reservoirs, typically defined as 30–100 m, balancing feasibility and potential in regions with moderate topography.

MISO Midcontinent Independent System Operator; a regional transmission organization (RTO) that coordinates electricity flow across parts of the central U.S., including Michigan.

NAD 1983 North American Datum of 1983; a geodetic reference system used for geographic coordinate positioning in North America.

NOAA National Oceanic and Atmospheric Administration; a U.S. federal agency providing environmental and water data, including lake level observations.

NREL National Renewable Energy Laboratory; a U.S. Department of Energy national lab specializing in renewable energy research.

Open-loop PHS A type of pumped hydro storage system that uses an existing natural water body (e.g., lake or river) as one of the two reservoirs, typically the lower one.

PHS Pumped Hydro Storage; a large-scale mechanical energy storage system that stores electricity by pumping water to a higher elevation and releasing it through turbines when needed.

Water head The vertical distance between the upper and lower reservoirs in a pumped hydro storage system, representing the potential energy available for storage or generation.

CRediT authorship contribution statement

Xin Shen: Writing – original draft, Visualization, Validation, Software, Resources, Methodology, Investigation, Formal analysis, Data curation, Conceptualization. **Jon W. Allan:** Writing – review & editing, Supervision, Resources. **Marc Gaden:** Writing – review & editing, Supervision. **Jeremy D. Bricker:** Writing – review & editing, Supervision, Resources, Project administration, Funding acquisition, Conceptualization.

Declaration of Generative AI and AI-assisted technologies in the writing process

During the preparation of this work, the authors used ChatGPT (OpenAI, GPT-4) solely to improve the readability and language of the manuscript. After using this tool, the authors reviewed and edited the content as needed and take full responsibility for the content of the published article.

Funding statement

This work was funded by a grant from the Carbon Neutrality Acceleration Program (CNAP) of the Graham Sustainability Institute at the University of Michigan.

Declaration of competing interest

The authors declare the following financial interests/personal relationships which may be considered as potential competing interests: Jeremy D. Bricker reports financial support was provided by Carbon Neutrality Acceleration Program (CNAP), Graham Sustainability Institute, University of Michigan. If there are other authors, they declare that they have no known competing financial interests or personal relationships that could have appeared to influence the work reported in this paper.

Appendix A. Detailed introduction

To avoid the worst impacts of rising global energy demand and increasing carbon dioxide emissions, decarbonization is imperative for the global economy [92]. In 2021, the U.S. The Department of State formally committed to achieving net-zero emissions by 2050 at the latest, as outlined in its Long-Term Strategy (LTS) submitted to the United Nations Framework Convention on Climate Change (UNFCCC) [93]. The report pledged to reduce U.S. greenhouse gas emissions by 50 % by 2030 in phases; however, by that time, the U.S. had achieved less than one-quarter of this target [94]. This significant lag in progress has rendered emission reduction efforts increasingly urgent and challenging.

To achieve net-zero emissions by 2050, a complete transformation of the global energy system is required. This is especially crucial because, prior to the recent push for transformation, electric power had been the largest sector contributing to U.S. greenhouse gas emissions, accounting for 30 % of emissions since 1990 (U.S. Environmental Protection Agency (EPA), 2022) [95]. The International Energy Agency (IEA) has emphasized that, in order for the electric power sector to fulfill its role in decarbonizing the energy system, the top priority is the transformation and enhancement of low-carbon supply. Renewable energy sources, such as wind and solar power, are key technologies for reducing emissions in the electric power sector due to their carbon-neutral nature [96]. According to IEA guidance, by 2050, solar photovoltaic (PV) capacity is projected to increase twentyfold, while wind power capacity is projected to increase elevenfold. At that point, approximately 90 % of electricity generation is projected to originate from renewable energy sources, with PV and wind collectively contributing nearly 70 % to the total [1]. Although this blueprint may seem ambitious, by 2020, renewable energy already accounted for 29 % of the global electricity supply, ranking as the second-largest contributor to the world-wide electricity mix [97]. Multiple studies have indicated that the global potential for renewable energy remains substantial, with wind and solar power being sufficient to meet the electricity demands of the world's leading economies ([98,99]).

As the energy system undergoes a growing reliance on renewable energy while the role of conventional thermal power declines, the focus of energy security will shift toward enhancing the flexibility of power systems to ensure a reliable supply [1]. The inherent intermittency and unpredictability of renewable energy will substantially increase the significance of utility-scale energy storage. Additionally, research indicates that the risk of power blackouts will significantly increase in the coming decades within the broader context of climate change [2,3]. Therefore, in order to prevent failures in other critical systems that rely on continuous power supply and to avoid cascading impacts across various sectors of the economy [4], ensuring the flexibility and reliability of power supply will become a critical challenge [5].

In the past decade, there has been a renewed global interest in Pumped Hydro Storage (PHS) technology. Unlike its expansion in the 1970s, which was driven by the need for load-leveling in nuclear baseload power [6], this time it is regarded as a mature, reliable, and rapidly responsive solution to address the intermittency of solar and wind power generation [13]. PHS is the most widely deployed and mature utility-scale energy storage technology, accounting for over 90 % of global utility-scale storage as of 2020 [12]. In the United States, it constitutes 70 % of utility-scale installed power capacity (MW) and 96 % of total energy storage capacity (MWh) [100]. According to the International Hydropower Association (IHA), a total of 9000 GWh of pumped hydro storage is currently available worldwide, with 161 GW of installed capacity already contributing to grid stability and reducing emissions in the power sector [7]. As the penetration of wind and solar energy continues to increase, an additional 78 GW of pumped hydro storage capacity is projected to be added globally by 2030 (IHA, 2018) [7] to enhance grid reliability and mitigate the growing curtailment of wind and solar energy caused by transmission constraints [101].

The dominance of pumped hydro storage in utility-scale energy storage is attributed to its technological, economic, and sustainability advantages, as well as its scalability [6,7]. After several decades of development, PHS has become the most mature commercial energy storage technology [10,15]. Its operational lifespan, which is several times longer than that of metal batteries, results in a significantly lower lifetime cost [11]. Many studies [9,10] have shown that PHS technology ranks among the most cost-effective energy storage technologies in terms of costs per kWh of electricity stored and produced, and it becomes even more cost-effective as it scales up. However, when scaled to the utility level, the frequent battery replacements and associated costs of waste battery disposal and recycling become a significant cost penalty for metal batteries [66], which also diminishes their competitiveness in terms of sustainability [102]. A direct indicator of sustainability is the Energy Storage on Investment (ESOI), which represents the ratio of the total energy stored over the lifetime of the storage system to the energy required for its construction. Study by Barnhart and Benson [8] shows that among all metal batteries, the highest ESOI is 32 for Li-ion, whereas PHS has an ESOI exceeding 700.

Despite the notable advantages that secure PHS a significant share among various energy storage technologies, topographical constraints have remained one of its primary drawbacks. A substantial elevation difference (water head) has long been a prioritized criterion for the siting and design of PHS projects [14]. Therefore, many countries and regions with flat terrain have had to exclude PHS from their energy storage portfolio [15]. The limited availability of suitable sites constrains the future growth of PHS capacity [16]. In fact, this traditional mindset regarding site selection has led to an underestimation of the potential and feasibility of PHS. Despite the maturity of PHS technology in mountainous areas, regions outside large mountain ranges have not yet developed PHS to their full potential. If the traditional PHS application range can be extended to low-head (2–30 m) and medium-head (30-100 m) systems, and the economic feasibility is demonstrated, large-scale low- and medium-head PHS can be integrated into regions where PHS has not been considered a viable solution so far [22]. Among the various configurations, open-loop PHS, which uses existing lakes or runoff-fed rivers as the lower reservoir and constructs only the upper reservoir artificially, offers a more accessible and commonly adopted solution. This approach is exemplified by the Ludington Pumped Hydro Storage Plant on the shore of Lake Michigan, the second-largest PHS facility in the United States. Operated by Consumers Energy, Ludington utilizes the lake as its lower reservoir and a man-made basin atop a coastal dune as its upper reservoir, delivering an installed capacity of 2172 MW and a total energy storage capacity of 19,548 MWh [24]. In this context, the Great Lakes is one such region with large natural basins as well as sufficient topography for traditional medium-head open-loop PHS, as well as offshore low-head open-loop PHS. The extensive shoreline of the Great Lakes and the diverse topographic conditions offer significant flexibility and feasibility for the development of low- and medium-head PHS. To achieve the goal of a net-zero economy by 2050, the U.S. grid will require approximately 270 GW of mechanical technologies, primarily based on PHS, to support inter-day Long Duration Energy Storage (LDES) (DOE, 2023) [83]. On a global scale, inter-day storage will require around 500 TWh of energy storage and 20 TW of capacity, which represents an order of magnitude increase compared to current levels [25]. Such a massive demand is unlikely to be met unless the traditional site selection limitations of PHS are overcome and its potential is re-explored. This is especially relevant given the past and near-future proliferation of wind power along and potentially within the lakes. Michigan currently has 2.5 GW of installed wind capacity, increasing rapidly on land. Considering the vast potential of lake-based wind power and its spatial compatibility with PHS, this co-location of energy generation with large-scale energy storage (just as Ludington PHS plant on Lake Michigan is co-located with nuclear generation) would allow efficient centralization of power transforming, switching, and transmission, making the time ripe for upscaling of PHS in this region.

At the same time, the concentration of wind power growth may bring to light the limitations of transmission capacity [28]. Network congestion-induced curtailment of wind energy could increase from 0.4 TWh in 2020 to 9.3 TWh by 2030, as simulated by the EU's Twenties project [29]. It is analyzed that, rather than building costly and time-intensive new transmission lines, a more effective solution is to store energy locally for time-shifting generation to maximize the utilization of this wind energy [30]. In addition, the design of low- and medium-head PHS plants allows for the use of more fish-friendly water pump and turbine technologies, such as the Archimedean screw, which can significantly reduce the impact on the ecological environment [89]. Considering the negative public perception of large-scale renewable energy projects [31,103], as well as the opposition of Michigan local communities to the commercial utilization of Great Lakes resources, low- and medium-head PHS plants might represent a balanced compromise between development and societal concerns.

Appendix B. Energy storage demand estimation for michigan

MISO (Midcontinent Independent System Operator) projects the generation fleet for 2039 based on its historical generation data and operational footprint [37]. In the highest storage demand scenario, the projected total energy (TWh), total capacity (GW), and the quantities of each resource of the entire operational footprint in 2039 are provided in Table B.1**.**

The storage capacity (GW) is distributed across 20 Local Resource Zones (LRZ) throughout the entire operational footprint, with Michigan consisting of part of LRZ 2 (Upper Peninsula) and LRZ 7 (Lower Peninsula). This allows us to calculate the storage capacity demand within Michigan and its proportion within the entire footprint. Energy of storage (GWh) in Michigan, although not specified separately as capacity, can be estimated from the total energy of storage across the entire footprint by assuming that the capacity proportions between Michigan and the entire footprint remain consistent. Table B.2 shows the storage capacity demand (GW) and the estimated energy demand (GWh) in Michigan and the proportions of the entire footprint.

PHS plants can operate (i.e. charge and discharge) on a daily to weekly basis depending on the demands of the power market. Different operating frequencies require varying storage capacities; Operating daily requires a smaller storage capacity, while operating weekly requires a larger one. In this study, the minimum energy storage demand (GWh) throughout Michigan is determined by assuming that all PHS plants operate on a daily basis. Conversely, the maximum demand is determined by assuming that these plants operate weekly. As established earlier, the annual total energy demand

Table B.1
Projected total energy, capacity, and resource quantities of the entire footprint.

Resource	Gas	Wind	Solar	Hybrid	Coal	Nuclear	Other	Storage	Total
Capacity (GW)	121	136	36	11	8	11	7	35	365
Energy (TWh)	420	526	65	31	0	89	74	147	1353

Table B.2
Storage capacity demand and estimated energy demand in Michigan and proportions of the entire footprint.

	Part of LRZ 2 (UP)	LRZ 7 (LP)	Michigan	Entire Footprint
Capacity (GW)	0.566*	6.068	6.634	35.400
Energy (GWh)	2350.339	25,197.627	27,547.966	147,000
Proportion	1.599 %	17.141 %	18.740 %	100 %

* This value was derived based on the total storage capacity of LRZ2 and the proportion represented by the two sites located in the Upper Peninsula out of the eleven sites in LRZ2.

in Michigan requiring storage is 27,547.97 GWh in 2039. The range of per-cycle energy demand across all PHS plants may be derived by dividing the annual demand by the operating frequency per year. For the results of energy storage demand calculations in Michigan, please refer to Table 2.1 in Section 2.1.

Appendix C. Legend of restricted areas and relevant case examples

The restricted area categories, legend, and data sources corresponding to Fig. 2.1 are provided in Table C.1.

It should be emphasized that the "restricted areas" considered in this study are based on preliminary and general expectations. However, this is not definitive; for instance, while national forests are repeatedly excluded in the mapping process due to the overlap with similar restricted areas (e.g. environmental areas), there are indeed several pumped hydro storage plants constructed on federal land in the United States, such as the Seneca Pumped Storage Project, located in the Allegheny National Forest [48]. Furthermore, these expectations are grounded in the current considerations of energy, environmental, and political circumstances, which may evolve as environmental issues intensify, energy demands increase, and energy structures change [49]. For example, the National Park Service (NPS) has implemented an assistance program to actively participate in Federal Energy Regulatory Commission (FERC) Hydropower Licensing Proceedings [105]. The U.S. Nuclear Regulatory Commission (NRC) is reviewing a proposal in 2023 regarding the potential reactivation of the Palisades Nuclear Plant (PNP) [88], which represents one of Michigan's possible options for energy transition. Although the plant is located in Covert, Michigan, within the high-risk erosion zones (primarily along the western shore of the Lower Peninsula) that are excluded in this study, it had previously operated smoothly for over 40 years before being decommissioned in 2022. This recent development suggests that high-risk erosion zones which have already been secured and have successfully hosted operational projects should not be categorically or permanently excluded. In fact, Michigan's most well-known and the second-largest PHS plant in the United States, the Ludington PHS Plant [24], is also located within such a high-risk erosion zone. The plant continues to operate steadily and plays an active role in Michigan's power system.

Table C.1
Categories of restricted areas.

Legend	Category	Data Source
	State Borders	USGS [46]
	Great Lakes Shoreline	ArcGIS [104]
	Search Zone (20 km inland)	–
	National Park Service	BLM [39]
	US Forest Service	BLM [39]
	US Fish and Wildlife	BLM [39]
	Bureau of Indian Affairs	BLM [39]
	Bureau of Land Management	BLM [39]
	Department of Defense	BLM [39]
	State Parks and Huntable Lands	EGLE [40]
	Land or Resource Use Constrain (due to contamination)	EGLE [41]
	Environmental Areas	EGLE [42]
	National Wetland Inventory (NWI) Plus	EGLE [43]
	High Risk Erosion Zones	EGLE [44,47]
	Cities Areas	EGLE [45]
	Biodiversity Protection (GAP Status 1&2)	USGS [46]
	Michigan State Easement	USGS [46]
	Inland Blocked Restricted Areas	–

Appendix D. Derivation of storage geometry, hydraulic losses, and energy storage calculation

This appendix presents the derivation of storage geometry, hydraulic loss formulation, and energy storage calculation consistent with the site configuration illustrated in Fig. 2.2 (Section 2.3).

Within each potential site, land elevation may vary. Therefore, "the elevation of the upper reservoir" is defined as the average land elevation within an identified site. The difference between this average elevation and the water level of the free lake surface represents the gross water head (gross water head, Eq. D.1) H_{gross}, which is the parameter used for the head threshold in previous sensitivity analysis.

$$H_{gross} = Elev_{site,avg} - Elev_{lake} \tag{D.1}$$

Meanwhile, "the depth of the upper reservoir" *Depth* is defined as twice the difference between the maximum and minimum elevations within the same site after construction, with symmetry around the average elevation. (Fig. 2.2) This is based on the assumption that the volume of excavation equals the volume of fill, in accordance with conventional practice of balancing cut and fill earthwork (Oglesby & Hicks, 1982) [106]. To prevent unreasonable depth and low head due to excessive elevation fluctuations, an additional threshold is considered necessary. The maximum depth of the upper reservoir is not permitted to exceed 30 % of its gross water head H_{gross} (15 % for excavation and 15 % for fill), based on the depth-to-head ratio at the Ludington Pumped Hydro Storage Plant. [24].

For practical operational considerations [107,108], the dead storage level and freeboard level are accounted for. The dead storage level H_{ds} is set at 9 % of the upper reservoir depth, representing an average value derived from studies of previous projects [107]. The freeboard level H_{fb}, which fluctuates during operation and is difficult to pinpoint precisely, is similarly set at 9 % of the depth for convenience in subsequent calculations. Therefore, the actual available heights of the upper reservoir—the heights above (filling) and below (excavating), symmetrically around the average elevation—are given by Eq. D.2 to Eq. D.4.

$$h_{above} = Depth - H_{fb}, \quad h_{below} = Depth - H_{ds} \tag{D.2}$$

$$h_{above} = h_{below} = 0.41\ Depth \tag{D.3}$$

$$s.t. Depth \leq 30\% H_{gross} \tag{D.4}$$

The actual available water head H_{av} refers to the elevation difference from the intake installation level. Since intakes must be installed above the dead storage level, the available head is therefore calculated by Eq. D.5 and Eq. D.6.

$$H_{av} = H_{gross} - h_{below} \tag{D.5}$$

$$H_{av} = Elev_{site,avg} - Elev_{lake} - 0.41 Depth \tag{D.6}$$

While the potential sites identified during the site identification process are generally irregular in shape, in engineering practice, upper reservoirs are typically constructed in circular [109], elliptical, or approximately elliptical [110] forms. Therefore, in this study, all potential sites are assumed to be circular, and an equivalent radius—defined as the radius of a circle with the same area as the site—is introduced as a characteristic parameter for subsequent calculations, i.e., the equivalent radius is given by Eq. D.7.

$$R_0 = \sqrt{A_0/\pi} \tag{D.7}$$

Here A_0 is the plan area of the site at the average elevation (km^2), also the area delineated during the site identification process; and R_0 is the equivalent radius corresponding to A_0 (km).

For safety considerations, both the inner and outer sides of the upper reservoir are typically constructed with a certain slope in engineering practice. In this study, the inner slope is set to a ratio of 1 vertical to 2.5 horizontal, based on the design of the Ludington plant [110].

Similar to the site area, the entire upper reservoir is assumed to be a frustum of a cone, with the equivalent radius of the top area R_{top}scaled up in proportion to the slope based on h_{above} , and equivalent radius of the bottom area R_{bottom} scaled down in proportion to the slope based on h_{below}. (The areas here refer to the volume excluding the dead storage level and freeboard level.) The relationship between $R_{top}$and R_{bottom} is given by Eq. D.8:

$$R_{top} = R_0 + 2.5 h_{above}, \quad R_{bottom} = R_0 - 2.5 h_{below} \tag{D.8}$$

These geometric parameters are then used to compute the actual available storage volume V_{av} using the formulation in Eq. 2.1 (Section 2.3).

For each identified site, the total energy storage capacity exists in the form of the gravitational potential energy of the water it holds, which can therefore be calculated by Eq. D.10:

$$E_{tot} = \rho \cdot g \cdot V_{av} \cdot H_{av} \cdot \eta_m \cdot 2.8 \times 10^{-13} \tag{D.10}$$

where, E_{tot} is the total energy storage capacity per cycle (GWh), ρ is the density of water (1000 kg/m^3), g is gravitational acceleration (9.81 m/s^2), V_{av} is the available volume of water in the upper reservoir (m^3), H_{av} is the available head (m), η_m is the round-trip efficiency of the system (assumed as 80 %), and 2.777778×10^{-13} is the unit conversion factor from Joules to Gigawatt-hours for consistency in the present study. The feasible energy storage capacity must account for friction losses, which are subtracted from the total energy storage capacity. Due to the anticipated long penstock connecting the upper reservoir and the lakes, energy losses are primarily attributed to friction, while minor losses are neglected. For each identified site, the length of the penstock needed is determined by the available head and the shortest distance from the shoreline, as the hypotenuse of a right triangle given by Eq. D.11:

$$L = \sqrt{H_{av}^2 + d^2} \tag{D.11}$$

Where L is the penstock length (m), H_{av} is the available head (m), and d is the shortest distance from the shoreline (m). The Darcy-Weisbach equation gives the linear friction losses in a closed pipe as Eq. D.12:

$$h_L = f \bullet {}^{L}/_{D} \bullet {}^{v^2}/_{2g} \tag{D.12}$$

Where h_L is the friction loss (m), f is the friction factor, L is the penstock length (m), D is the internal diameter of the penstock (m), v is the inside flow velocity, and g is gravitational acceleration (9.81 m/s^2). The friction factor f is given by the Colebrook – White equation (Colebrook, 1939) as Eq. D.13:

$$f = \frac{0.25}{\left[log\left({}^{\epsilon}/_{3.7D} + {}^{5.74}/_{Re^{0.9}}\right]^2} \tag{D.13}$$

Where ϵ is the relative roughness (0.076 mm for commercial steel), and Re is the Reynolds number.

The frictional energy loss (GWh) per storage cycle, derived from the friction loss described in Eq. D.12, can be calculated as Eq. D.14:

$$E_{Loss} = \rho \cdot g \cdot V_{av} \cdot h_L \cdot 2.777778 \times 10^{-13} \tag{D.14}$$

Accordingly, the feasible energy storage $E_{feasible}$ is obtained by subtracting the frictional energy loss E_{Loss} from the total potential energy E_{tot}, as given in Eq. 2.2.

Note that friction losses are determined by the penstock diameter, as the friction factor f and flow velocity v are functions of it. However, without additional design constraints, the diameter cannot be uniquely determined. Therefore, an optimization process is necessary to determine the penstock diameter that minimizes friction losses. As the optimization also involves considerations of penstock cost, this topic is discussed in Section 2.4.2.

Appendix E. Detailed discussion of selling/buying periods, period-average LMPs, and arbitrage calculations

Arbitrage is indicated to be related to price dynamics, duration of storage, and the round-trip efficiency of the plants [58], among other factors. A study by Thomas Nguyen Mercier et al. [58] evaluated energy storage in the power markets of the 28 EU countries. The findings indicate that the marginal value of additional storage becomes negligible after 4 to 6 h of duration. Therefore, in conjunction with the MISO report on the pumping operation of the Ludington PHS plant [59], the present study sets the generating-selling period for all identified PHS plants to 6 h and the pumping-buying period to 8 h, assuming that electricity selling needs to occur within a more compact time span.

In this study, the price taker model will be adhered to, assuming that PHS plants do not possess any market power to influence electricity prices in the power market, even though storage is assumed to contribute a certain share of energy supply [111]. In previous arbitrage estimation models [57,60], the highest price hour within a day is typically considered the beginning of the selling period, and the lowest price hour is considered the beginning of the buying period. However, it is unlikely that the price in the following hours will remain relatively high or low, given the fluctuation of LMP. Therefore, based on the time spans defined earlier, this study identifies the selling period as the 6 h in which the period-averaged hourly LMP within the whole time span is the highest, while the buying period is defined as the 8 h in which the hourly average LMP is the lowest.

The long-term hourly average LMP values on a daily basis are calculated from historical Michigan Hub LMP data on MISO for the period April 2024 to August 2024 [55,61] The hourly average LMP, along with the selling and buying periods and their corresponding period-specific average LMP, are presented Fig. E.1.

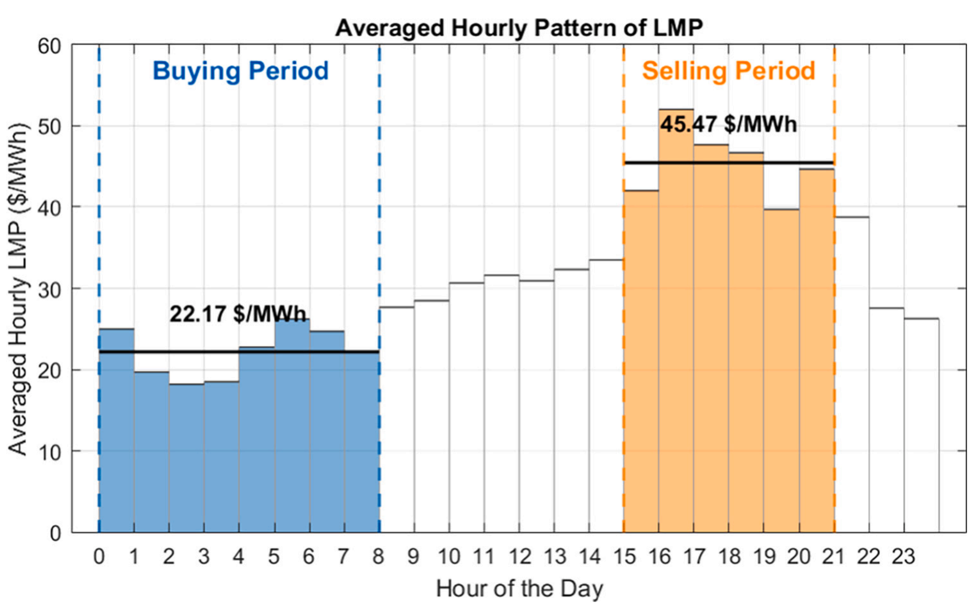

Fig. E.1. Averaged hourly pattern of LMP with selling and buying periods.

The revenue in each cycle (daily) is the product of the energy sold during the selling period and the corresponding period-averaged LMP, while the cost is the product of the energy bought during the buying period and the corresponding period-averaged LMP. The arbitrage profit is defined as the difference between these two values, as illustrated in Eq. E.1, Eq. E.2 and Eq. E.3:

$$R = E_{feasible} \times LMP_s \tag{E.1}$$

$$C = E_{feasible} \times LMP_b \tag{E.2}$$

$$P = R - C \tag{E.3}$$

Where $E_{feasible}$ is the feasible energy storage capacity (converted into MWh) (assumed be sold out), LMP_s is the period-average LMP for the selling period ($/MWh), LMP_b is the period-average LMP for the buying period ($/MWh), R is the revenue per cycle ($/day), C is the cost per cycle ($/day) and P is the arbitrage profit per cycle ($/day).

Appendix F. Calculation process for optimal penstock diameter

The cost of long penstocks and the associated friction loss are significant components of the economic analysis. For large identified feasible reservoirs, it is nearly impossible to meet the substantial discharge required during operation with a single penstock. Consequently, the number of penstocks n is introduced as a new variable and is interrelated with penstock diameter D, which makes it impossible to determine an optimal diameter without additional constraints. (as discussed in section 2.3.3).

Economic analysis provides the appropriate context for optimizing penstock diameter: while an increase in diameter raises construction and maintenance costs, it reduces friction loss along the penstock, as well as the subsequent energy loss and revenue loss. In this section, the increasing costs and decreasing losses will be estimated and quantified as functions of penstock diameter, with their intersection indicating the optimal diameter (economic diameter) D*.

Engineering conventions that are widely accepted in practice are introduced to constrain the range of variables in the optimization process:

1) The diameter of penstocks should be less than 3.5 m due to transportation constraints.
2) Flow velocity within the penstock should be greater than 3 ft./s to avoid sediment accumulation, but less than 15 ft./s to avoid scoring. In the optimization process, the inner velocity is consistently set to be the maximum acceptable value, i.e. 15 ft./s or 4.5 m/s, which is a practical assumption that ensures the minimum diameter among all optimal solutions.

Kumar and Singal (2015) evaluated the performance of five commonly used penstock materials, including commercial steel, using MADM methods [112]. Given that the penstock parameters in the cases they studied are similar to the aforementioned conventions, the steel-related findings from the evaluation are used to develop the relationship between penstock diameter and construction and maintenance costs, as Eq. F.1 and Eq. F.2:

$$CC_{penstock} = 49.553\,D^2 + 69.927\,D + 9 \times 10^{-13} \tag{F.1}$$

$$MC_{penstock} = 2.9724\,D^2 + 4.197\,D + 9 \times 10^{-14} \tag{F.2}$$

Where $CC_{penstock}$ is the construction cost of penstocks ($/m), $MC_{penstock}$ is the maintenance cost of penstocks ($/m/y) and D is the penstock diameter (m).

Friction losses occur during both the generating and pumping processes. The friction loss during generating is given by the Darcy-Weisbach equation as Eq. F.3:

$$h_{L.gen} = f \bullet {}^{L}\!/_{D} \bullet {}^{v^2}\!/_{2g} \tag{F.3}$$

Where $h_{L.gen}$ is the friction loss during generating (m), f is the friction factor given by Colebrook – White equation (E. D.13), L is the penstock length (m), D is the internal diameter of the penstock (m), v is the inside flow velocity (4.5 m/s), and g is gravitational acceleration (9.81 m/s^2).

The friction loss during pumping is derived from the ratio of the friction loss during generating.

Given that the generating period is 6 h and pumping period is 8 h, the flow velocity in the penstock during the two periods is inversely proportional to the duration of the periods, and the friction loss generated is inversely proportional to the square of the flow velocity, as Eq. F.4:

$$h_{L.pump} = {}^{9}\!/_{16} \times h_{L.gen} \tag{F.4}$$

Where $h_{L.pump}$ is the friction loss during pumping (m), and $h_{L.gen}$ is the friction loss during generating (m).

The total friction loss on the penstock is the sum of both friction losses, as Eq. F.5:

$$h_L = h_{L.gen} + h_{L.pump} \tag{F.5}$$

Where h_L is the total friction loss (m) and is also used in (eq. 2.2) to calculate the energy loss in each cycle. Thus Eq. D.14 can also be written as Eq. F.6:

$$E_L = \rho \cdot g \cdot V_{av} \cdot (h_{L.gen} + h_{L.pump}) \cdot 2.777778 \times 10^{-13} \tag{F.6}$$

The revenue loss due to friction loss can be further given by Eq. F.7:

$$R_{loss} = E_L \times LMP_s \tag{F.7}$$

Where R_{loss} is the revenue loss due to friction loss ($/d), E_L is the energy loss per cycle (GWh/d) and LMP_s is the period-averaged LMP in selling period.

The optimal diameter (economic diameter) may be indicated by the intersection of cost curves (Eq. F.1 and Eq. F.2) and the revenue loss curve. To facilitate the optimization process, the total economic cost $T(D)$ is defined as the sum of cost curves and revenue loss curve, as Eq. F.8:

$$T(D) = CC_{penstock}(D) + MC_{penstock}(D) + R_{loss}(D) \tag{F.8}$$

The optimal diameter D^* corresponds to the value of D that minimizes the total cost $T(D)$.This is represented as Eq. F.9, Eq. F.10 and Eq. F.11:

$$D^* = \underset{D}{argmin}\,T(D) \tag{F.9}$$

$$s.t.\;\; D \leq 3.5\,m \tag{F.10}$$

$$3\,ft/s < v < 15\,ft/s \tag{F.11}$$

The optimal diameter will be used to determine the final total friction loss by Eq. F.3, Eq. F.4 and Eq. F.5, the revenue loss by Eq. F.7, and the penstock costs by Eq. F.1 and Eq. F.2.

Appendix G. LCOE And LCOS calculations: formulas, parameters, and parameter rationale

Levelized Cost of Energy (LCOE) is a metric used to quantify the average cost per unit of energy produced by an energy system over its entire lifecycle, calculated by discounting the cumulative costs and dividing it by the total discounted energy output [62]. This methodology was originally established by Lazard in 2015 [63,64]. LCOE includes not only the costs incurred solely by the energy storage system, such as expenses related to construction and manufacturing (capital expenditures) and annual operation and maintenance (operating expenditures), but also additional charging costs, which are analogous to fuel costs in LCOE calculated for energy generation technologies. The calculation of LCOE is as Eq. G.1:

$$LCOE = \frac{CAPEX + \sum_{t=1}^{n} \frac{OPEX_t + C_{charing,t}}{(1+r)^t}}{\sum_{t=1}^{n} \frac{E_{annual,t}}{(1+r)^t}} \tag{G.1}$$

Where:

$CAPEX$ is the total capital expenditures ($);
$OPEX_t$ is the annual total operating expenditures in year t ($/yr);
$C_{charing,t}$ is the annual total charging cost in year t ($/yr);
$E_{annual,t}$ is the annual total energy generation in year t (MWh/yr);
r is the discount rate (%);
n is the operational lifetime of PHS plants (yr);
t is the year of lifetime (1, 2, …n).

Another commonly used cost metric specific to energy storage systems is the Levelized Cost of Storage (LCOS), which aims to quantify the average cost per unit of energy discharged from the storage system over its entire lifecycle. The definition of LCOS remains inconsistent across current studies [113,114], often resulting in confusion with LCOE. This approach draws from studies on Life Cycle Analysis (LCA) [68,115]. It is meaningful to isolate LCOS values, considering that the storage plants studied operate independently, rather than being attached to power generation plants.

As LCOS reflects the costs incurred solely by the energy storage system, it is derived by subtracting the annual charging costs from LCOE, as shown in Eqn. G. 2 and Eqn. G. 3:

$LCOS = \frac{CAPEX + \sum_{t=1}^{n} \frac{OPEX_t}{(1+r)^t}}{\sum_{t=1}^{n} \frac{E_{annual,t}}{(1+r)^t}}$ (G. 2).

$i.e. LCOE = LCOS + C_{charging,t}$ (G. 3).

The parameters are the same as those in the LCOE calculation.

All parameters for the LCOS and LCOE calculations are listed in Table G.1. The parameters of costs are listed on a per-unit basis (per kWh or per MWh), and require conversion to total annual values for use in the calculation:

For an identified PHS plant, the total capital expenditures $CAPEX$, considered to occur only before the operation, is the product of the unit construction costs (listed in Table G.1) and the feasible energy storage $E_{feasible}$. Assuming identified PHS plants operate on a daily basis, the annual total energy generation $E_{annual,t}$ will be the product of feasible storage $E_{feasible}$ and the operating times (365 days in a year). Thus, the annual total operating expenditures $OPEX_t$ and the annual total charging cost $C_{charing,t}$ are calculated by multiplying the corresponding unit costs (listed in Table G.1) by the annual total energy generation, without the need to introduce additional notations or formulas.

The sources and rationale for the data selection are presented below:

Chen (1990) analyzed the construction costs of PHS plants built and operational between 1963 and 1985 [116]. Additionally, Kendall Mongird et al. (2020) projected various costs of PHS technologies in 2030 in their assessment of energy storage technologies [117]. By combining the trends identified in Chen's (1990) analysis [116] with the cost projections from Kendall Mongird et al. [117], the maximum values across various cost categories within the predicted range were selected. These conservative estimates were selected considering the challenges of construction in the

Table G.1
Parameters of LCOS and LCOE calculations.

Notations	Parameters	Values
Capital Expenditures $CAPEX$	Reservoir Construction and Infrastructure ($/kWh)	70
	Powerhouse Construction and Infrastructure ($/kW)	686
	Electro-mechanical ($/kW)	392
	Contingency Fee ($)	33 %*
Operating Expenditures $OPEX$	Fixed Operations and Maintenance ($/kW/yr)	17.8
	Variable Operations and Maintenance ($/MWh)	8.0125
	System RTE losses ($/kWh)	0.0075
$C_{charing}$	Charging Cost ($/MWh)	22.17
r	Discount Rate (%)	7.60
t	Lifetime (yr)	40

* 33 % ratio of total capital costs.

mountainous northern Upper Peninsula, where the majority of potential sites identified during the primary site identification process are located. The contingency fee is essential for PHS projects due to their technological complexity and long construction periods. It is calculated as a proportion of total capital costs, with a 33 % ratio adopted from the report by Kendall Mongird et al. (2020) [117].

Charging cost is represented by the period-average LMP for the buying period LMP_b(calculated in Section 2.4.1). This is a simplified assumption that ignores commonly considered factors such as the Depth of Discharge (DoD) and the charging cost escalator [63]. Notice that the period-averaged LMP remains an estimate. Given the broad footprint of this study (the entire Michigan Shoreline), real-time LMPs exhibit significant variation [65].

The discount rate is determined to be 7.6 %, based on the assessment by Kendall Mongird et al. (2020) [117], which results in a higher and more conservative LCOS. The lifetime of PHS plants is set at 40 years based on the same assessment. However, the actual lifetime could be much longer, potentially resulting in a lower LCOS.

Data availability

The dataset generated and analyzed in this study, including the spatial locations and attributes of potential PHS sites in Michigan, as well as the ArcGIS processing workflow and the MATLAB script used for data analysis, are available in the Deep Blue Data repository at the University of Michigan: doi:https://doi.org/10.7302/y1q8-9p52.

References

[1] IEA, in: IEA (Ed.), Net Zero by 2050, Paris, 2021. https://www.iea.org/reports/net-zero-by-2050.

[2] S. Matthewman, H. Byrd, Blackouts: a sociology of electrical power failure, Social Space (Przestrzeń Społeczna) (2013) 31–55. https://hdl.handle.net/10779/lincoln.24334558.v1.

[3] D. Burillo, M.V. Chester, B. Ruddell, N. Johnson, Electricity demand planning forecasts should consider climate non-stationarity to maintain reserve margins during heat waves, Appl. Energy 206 (2017) 267–277, https://doi.org/10.1016/j.apenergy.2017.08.141.

[4] S.M. Rinaldi, J.P. Peerenboom, T.K. Kelly, Identifying, understanding, and analyzing critical infrastructure interdependencies, IEEE Control. Syst. Mag. 21 (6) (2001) 11–25, https://doi.org/10.1109/37.969131.

[5] M.V. Chester, B. Allenby, Toward adaptive infrastructure: Flexibility and agility in a non-stationarity age, Sustain. Resilient Infrastruct. 4 (4) (2019) 173–191, https://doi.org/10.1080/23789689.2017.1416846.

[6] J.P. Hoffstaedt, D.P.K. Truijen, J. Fahlbeck, L.H.A. Gans, M. Qudaih, A.J. Laguna, J.D.M. De Kooning, K. Stockman, H. Nilsson, P.-T. Storli, B. Engel, M. Marence, J. D. Bricker, Low-head pumped hydro Storage: A review of applicable Technologies for Design, grid integration, control and modelling, Renew. Sust. Energ. Rev. 158 (2022) 112119, https://doi.org/10.1016/j.rser.2022.112119.

[7] IHA, The World's Water Battery: Pumped Hydropower Storage and the Clean Energy Transition, International Hydropower Association (2018), IHA working paper, December 2018, https://www.hydropower.org/publications/the-world-e2-80-99s-water-battery-pumped-hydropower-storage-and-the-clean-energy-transition.

[8] C.J. Barnhart, M. Dale, A.R. Brandt, S.M. Benson, The energetic implications of curtailing versus storing solar- and wind-generated electricity, Energy Environ. Sci. 6 (2013) 2804–2810, https://doi.org/10.1039/C3EE41973H.

[9] V. Jülch, Comparison of electricity Storage options using Levelized cost of Storage (LCOS) method, Appl. Energy 183 (2016) 1594–1606, https://doi.org/10.1016/j.apenergy.2016.08.165.

[10] H. Chen, T.N. Cong, W. Yang, C. Tan, Y. Li, Y. Ding, Progress in electrical energy Storage system: A critical review, Prog. Nat. Sci. 19 (3) (2009) 291–312, https://doi.org/10.1016/j.pnsc.2008.07.014.

[11] M.M. Rahman, A.O. Oni, E. Gemechu, A. Kumar, Assessment of energy Storage technologies: A review, Energy Convers. Manag. 223 (2020) 113295, https://doi.org/10.1016/j.enconman.2020.113295.

[12] IHA, Hydropower Status Report, International Hydropower Association. (2021). https://www.hydropower.org/publications/2021-hydropower-status-report, 2021.

[13] M. Guittet, M. Capezzali, L. Gaudard, F. Romerio, F. Vuille, F. Avellan, Study of the drivers and asset Management of Pumped-Storage Power Plants: Historical and geographical perspective, Energy 111 (2016) 560–579, https://doi.org/10.1016/j.energy.2016.04.052.

[14] IEA and DOE, Implementing Agreement for a Co-operative Programme on Hydropower Technologies and Programmes, *as amended to 21 March* 2006, https://www.energy.gov/node/4813070, 2006.

[15] R. Ansorena Ruiz, L.H. de Vilder, E.B. Prasasti, M. Aouad, A. De Luca, B. Geisseler, K. Terheiden, S. Scanu, A. Miccoli, V. Roeber, M. Marence, R. Moll, J.D. Bricker, N. Goseberg, Low-head pumped hydro Storage: A review on civil structure designs, legal and environmental aspects to make its realization feasible in seawater, Renew. Sust. Energ. Rev. 160 (2022) 112281, https://doi.org/10.1016/j.rser.2022.112281.

[16] M. Semadeni, Energy Storage as an essential part of sustainable energy systems: A review on applied energy Storage technologies, CEPE Working Paper 24 (2003), https://doi.org/10.3929/ethz-a-004532521.

[17] N. Ghorbani, H. Makian, C. Breyer, A GIS-based method to identify potential sites for pumped hydro energy Storage - case of Iran, Energy 169 (2019) 854–867, https://doi.org/10.1016/j.energy.2018.12.073.

[18] J. Li, D. Chen, W. Han, P. Wang, Z. Zhao, G. Liu, Site identification and capacity determination of pumped hydro storage plants using GIS and spatial MCDM in Northwest China, Energy Convers. Manag. 322 (2024) 119179, https://doi.org/10.1016/j.enconman.2024.119179.

[19] D. Connolly, S. MacLaughlin, M. Leahy, Development of a computer program to locate potential sites for pumped hydroelectric energy storage, Energy 35 (1) (2010) 375–381, https://doi.org/10.1016/j.energy.2009.10.004.

[20] N. Fitzgerald, R. Lacal Arántegui, E. McKeogh, P. Leahy, A GIS-based model to calculate the potential for transforming conventional hydropower schemes and non-hydro reservoirs to pumped hydropower schemes, Energy 41 (1) (2012) 483–490, https://doi.org/10.1016/j.energy.2012.02.044.

[21] S. Kucukali, Finding the most suitable existing hydropower reservoirs for the development of pumped-storage schemes: An integrated approach, Renew. Sust. Energ. Rev. 37 (2014) 502–508, https://doi.org/10.1016/j.rser.2014.05.052.

[22] J.P. Hoffstaedt, D.P.K. Truijen, J. Fahlbeck, L.H.A. Gans, M. Qudaih, A.J. Laguna, J.D.M. De Kooning, K. Stockman, H. Nilsson, P.-T. Storli, B. Engel, M. Marence, J. D. Bricker, Low-head pumped hydro Storage: A review of applicable Technologies for Design, grid integration, control, and modelling, Renew. Sust. Energ. Rev. 158 (2022) 112119, https://doi.org/10.1016/j.rser.2022.112119.

[23] National Renewable Energy Laboratory (NREL), *Pumped Storage Hydropower*, (accessed 2025). https://maps.nrel.gov/psh.

[24] Wikipedia contributors, Ludington Pumped Storage Power Plant, *Wikipedia*, (accessed 2024) https://en.wikipedia.org/wiki/Ludington_Pumped_Storage_Power_Plant.

[25] A. Blakers, M. Stocks, B. Lu, C. Cheng, A review of pumped hydro energy Storage, Progress in Energy. 3 (2021) 022003, https://doi.org/10.1088/2516-1083/abeb5b.

[26] A. Adelaja, C. McKeown, B. Calnin, Y. Hailu, Assessing offshore wind potential, Energy Policy 42 (2012) 191–200, https://doi.org/10.1016/j.enpol.2011.11.072.

[27] NREL, *Michigan 50-Meter Community-Scale Wind Resource Map*, (accessed 2025) https://windexchange.energy.gov/maps-data/61.

[28] D.J. Burke, M.J. O'Malley, Factors influencing wind energy curtailment, IEEE Transactions on Sustainable Energy. 2 (2) (2011) 185–193, https://doi.org/10.1109/TSTE.2011.2104981.

[29] Red Eléctrica de España, Transmission System Operation with a Large Penetration of Wind and Other Renewable Electricity Sources in Electricity Networks Using Innovative Tools and Integrated Energy Solutions (TWENTIES), TWENTIES Project Final Report - Short Version. (2013) June, red Eléctrica de España, Iberdrola, Gamesa, COMILLAS-IIT, DONG Energy, Fraunhofer IWES, energinet. Dk, RTE, Alstom grid, INESC Porto, University College Dublin, University of Strathclyde, Siemens wind power, SINTEF energy research, Elia, ABB, and 50Hertz,http://www.ewea.org/fileadmin/files/library/publications/reports/Twenties_report_short.pdf.

[30] M. Moradzadeh, B. Zwaenepoel, J. Van de Vyver, L. Vandevelde, Congestion-induced Wind Curtailment Mitigation Using Energy Storage, IEEE international energy conference (ENERGYCON), Cavtat, Croatia 2014 (2014) 572–576, https://doi.org/10.1109/ENERGYCON.2014.6850483.

[31] T.M. Groth, C. Vogt, Residents' perceptions of wind turbines: An analysis of two townships in Michigan, Energy Policy 65 (2014) 251–260, https://doi.org/10.1016/j.enpol.2013.10.055.

[32] L. Graham, A Change in Power, Part 3: Storing energy to use later, Michigan Public (2025 April 16). https://www.michiganpublic.org/environment-climate-change/2025-04-16/a-change-in-power-part-3-storing-energy-to-use-later.

[33] National Wildlife Federation v. Consumers Power Co., 657 F. Supp. 989 (W.D. Mich. 1987), March 31, 1987, no. G85–1146, United States District Court for the Western District of Michigan. https://law.justia.com/cases/federal/district-courts/FSupp/657/989/2265156/.

[34] C.A. Jones, An economic model to assess fish-kill damages, Resources Magazine. https://www.resources.org/archives/an-economic-model-to-assess-fish-kill-damages/, 1989 October.

[35] J. Görtz, M. Aouad, S. Wieprecht, K. Terheiden, Assessment of pumped hydropower energy Storage potential along Rivers and shorelines, Renew. Sust. Energ. Rev. 165 (2022) 112027, https://doi.org/10.1016/j.rser.2021.112027.

[36] R. Arantegui, N. Fitzgerald, P. Leahy, Pumped-Hydro Energy Storage: Potential for Transformation from Single Dams, Publications Office of the European Union, 2012, https://doi.org/10.2790/44776. EUR 25239 EN, JRC68678.

[37] MISO, *Futures Report*, Published April 2021 - Updated. https://cdn.misoenergy.org/MISO%20Futures%20Report538224.pdf, December 2021.

[38] USGS, EarthExplorer (accessed 2024), https://earthexplorer.usgs.gov/.
[39] Bureau of Land Management (BLM), National Data Viewer, (accessed 2024). https://experience.arcgis.com/experience/9a89ee80c604431e8f8d939a186fbdbb.
[40] Michigan Dept. Oof eEnvironment, Great Lakes, and eEnergy (EGLE), Land or Resource Use Restriction (Polygons). https://gis-egle.hub.arcgis.com/datasets/egle::land-or-resource-use-restriction-polygons/about, 2023.
[41] EGLE, Land or Resource Use Restriction (Polygons). https://gis-michigan.opendata.arcgis.com/datasets/6bfc773ae55241ce85736528fb21a0cd_5/about, 2023.
[42] EGLE, Environmental Areas. https://gis-egle.hub.arcgis.com/datasets/egle::environmental-areas/about, 2021.
[43] EGLE, National Wetland Inventory (NWI) Plus 2005. https://gis-egle.hub.arcgis.com/datasets/egle::national-wetland-inventory-nwi-plus-2005/about, 2021.
[44] EGLE, High Risk Erosion Zones, 2021. https://gis-egle.hub.arcgis.com/datasets/egle::high-risk-erosion-zones/about.
[45] EGLE, Remediation Information Data Exchange (RIDE) Mapper (accessed 2024), https://www.michigan.gov/egle/maps-data/ride-mapper.
[46] USGS, The Protected Areas Database of the United States (PAD-US) (accessed 2024), https://maps.usgs.gov/padusdataexplorer/#/protected-areas.
[47] Legal Information Institute, *Mich. Admin. Code R. 281.22 - High-risk erosion areas*, (accessed 2024). https://www.law.cornell.edu/regulations/michigan/Mich-Admin-Code-R-281-22.
[48] Hydropower Reform Coalition, Seneca P-2280 (accessed 2024), https://hydroreform.org/hydro-project/seneca-p-2280/.
[49] M.T. Craig, S. Cohen, J. Macknick, C. Draxl, O.J. Guerra, M. Sengupta, S.E. Haupt, B.-M. Hodge, C. Brancucci, A review of the potential impacts of climate change on bulk power system planning and operations in the United States, Renew. Sust. Energ. Rev. 98 (2018) 255–267, https://doi.org/10.1016/j.rser.2018.09.022.
[50] National Oceanic and Atmospheric Administration (NOAA), CO-OPS Map - NOAA Tides & Currents (accessed 2024), https://tidesandcurrents.noaa.gov/map/index.html.
[51] B. Nelson-Mercer, H. Tomkins, T. Ahsan, C. Troy, Beach rebuilding period buffers Indiana Beach erosion in Lake Michigan, J. Great Lakes Res. (102226) (2023), https://doi.org/10.1016/j.jglr.2023.08.003. In press, Corrected Proof.
[52] B. Lu, M. Stocks, A. Blakers, K. Anderson, Geographic information system algorithms to locate prospective sites for pumped hydro energy Storage, Appl. Energy 222 (2018) 300–312, https://doi.org/10.1016/j.apenergy.2018.03.177.
[53] T.M. Groth, C. Vogt, Residents' perceptions of wind turbines: An analysis of two townships in Michigan, Energy Policy 65 (2014) 251–260, https://doi.org/10.1016/j.enpol.2013.10.055.
[54] B. Solis, Wind Farm East of Muskegon Met with Lawsuits, Recall Attempts, MLive. https://www.mlive.com/news/muskegon/2019/08/wind-farm-east-of-muskegon-met-with-lawsuits-recall-attempts.html, 2019.
[55] W.W. Hogan, Contract networks for electric power transmission, J. Regul. Econ. 4 (1992) 211–242, https://doi.org/10.1007/BF00133621.
[56] P.L. Joskow, Lessons learned from electricity market liberalization, Energy J. 29 (2_suppl) (2008), https://doi.org/10.5547/ISSN0195-6574-EJ-Vol29-NoSI2-3.
[57] D. Connolly, H. Lund, P. Finn, B.V. Mathiesen, M. Leahy, Practical operation strategies for pumped hydroelectric energy Storage (PHES) utilizing electricity Price arbitrage, Energy Policy 39 (2011) 4189–4196, https://doi.org/10.1016/j.enpol.2011.04.032.
[58] T.N. Mercier, Techno-Economics of Variable-Speed Pumped Hydro Energy Storage, PhD Thesis, Université Laval, Québec, Canada, and Université catholique de Louvain, Louvain-la-Neuve, Belgium, 2024. https://corpus.ulaval.ca/entities/publication/2e77978d-12dc-40a9-9446-ecd30cf7be56. Supervised by M. Olivier and E. De Jaeger.
[59] D. Bhatnagar, J.C. Bedoya, D.S. Boff, A. Somani, J. Twitchell, Compensation Mechanisms for Long Duration Energy Storage, Pacific Northwest National Laboratory, August 2022. PNNL-32978. DOE, https://www.pnnl.gov/main/publications/external/technical_reports/PNNL-32978.pdf.
[60] D. Zafirakis, K.J. Chalvatzis, G. Baiocchi, G. Daskalakis, The value of arbitrage for energy Storage: Evidence from European electricity markets, Appl. Energy 184 (2016) 971–986, https://doi.org/10.1016/j.apenergy.2016.05.047.
[61] ENERGYONLINE, MISO Actual Energy Price (accessed 2024), http://www.energyonline.com/Data/GenericData.aspx?DataId=8.
[62] C. Kost, J.N. Mayer, J. Thomsen, N. Hartmann, C. Senkpiel, S. Philipps, S. Nold, S. Lude, N. Saad, T. Schlegl, Levelized Cost of Electricity - Renewable Energy Technologies, Fraunhofer ISE, Freiburg/Brsg, 2012, p. 47 S, https://doi.org/10.24406/publica-fhg-296653.
[63] Lazard, Levelized Cost of Storage Analysis—Version 7.0, Lazard, 2021. https://www.lazard.com/media/42dnsswd/lazards-levelized-cost-of-storage-version-70-vf.pdf.
[64] C. Martínez de León, C. Ríos, P. Molina, J.J. Brey, Levelized cost of Storage (LCOS) for a hydrogen system, Int. J. Hydrog. Energy 52, Part A (2024) 1274–1284, https://doi.org/10.1016/j.ijhydene.2023.07.239.
[65] MISO, Markets and Operations, RT and Market Data, Markets Displays (accessed 2024), https://www.misoenergy.org/markets-and-operations/real-time–market-data/markets-displays/.
[66] A. Immendoerfer, I. Tietze, H. Hottenroth, T. Viere, Life-cycle impacts of pumped hydropower Storage and battery Storage, Nat. Energy 8 (2017) 231–245, https://doi.org/10.1038/s41560-017-0029-9.
[67] O. Torres, Life Cycle Assessment of a Pumped Storage Power Plant, *Master's Thesis*,, Norwegian University of Science and Technology, 2011, https://ntnuopen.ntnu.no/ntnu-xmlui/bitstream/handle/11250/234503/455355_FULLTEXT01.pdf?sequence=2&isAllowed=y.
[68] Guo, Z., Ge, S., Yao, X., Li, H., & Li, X., Life cycle sustainability assessment of pumped hydro energy storage, Int. J. Energy Res. (2019) 43, no. 14, doi:https://doi.org/10.1002/er.4890.
[69] M.F. Bonamusa, Life Cycle Assessment of Offshore Low Head Pumped Hydro Storage, *Master Thesis*, Delft University of Technology. https://resolver.tudelft.nl/2497f1ad-206a-4aeb-914d-cecff1ecb851, 2023.
[70] T.R. Simon, D. Inman, R. Hanes, G. Avery, D. Hettinger, G. Heath, Life cycle assessment of closed-loop pumped Storage hydropower in the United States, Environ. Sci. Technol. 57 (33) (2023) 12251–12258, https://doi.org/10.1021/acs.est.2c09189.
[71] U.S. Energy Information Administration (EIA), Michigan State Energy Profile (accessed 2025), https://www.eia.gov/state/analysis.php?sid=MI.
[72] NREL, Michigan High Resolution Wind Resource. https://catalog.data.gov/dataset/michigan-high-resolution-wind-resource-78e8c, 2025.
[73] A. Boezaart, J. Edmonson, C. Standridge, N. Pervez, N. Desai, B. Williams, A. Clark, D. Zeitler, S. Kendall, B. Biddanda, A. Steinman, B. Klatt, J.L. Gehring, K. Walter, E.E. Nordman, Lake Michigan offshore wind feasibility assessment, Grand Valley State University. (2014), https://doi.org/10.2172/1148917.
[74] A. Manocha, G. Mantegna, N. Patankar, J.D. Jenkins, Reducing transmission expansion by co-optimizing sizing of wind, solar, storage and grid connection capacity, Environmental Research: Energy. 2 (1) (2025) 015011, https://doi.org/10.1088/2753-3751/adafab.
[75] P. Denholm, Transmission Benefits of co-Locating Concentrating Solar Power and Wind, NREL, 2012, https://doi.org/10.2172/1036364.
[76] L. Forsberg, Negative prices in the MISO market: What's happening and why should we care?, in: *fresh energy* policy Report, 2018 November 15. https://fresh-energy.org/negative-prices-in-the-miso-market-whats-happening-and-why-should-we-care.
[77] American Transmission Company, LLC et al., 2025 Biennial Transmission Projects Report, *Minnesota Public Utilities Commission* Joint Utility Filing. (2025) October 31, MPUC Docket No. E999/M-25-99, https://www.minnelectrans.com/reports.html.
[78] Argonne National Laboratory, Pumped Storage hydropower: Benefits for grid reliability and integration of variable renewable energy, in: DOE, 2014. https://www.anl.gov/esia/pumped-storage-hydropower-benefits-for-grid-reliability-and-integration-of-variable-renewable-energy.
[79] M.H. Mostafa, S.H.E. Abdel Aleem, S.G. Ali, Z.M. Ali, A.Y. Abdelaziz, Techno-economic assessment of energy storage systems using annualized life cycle cost of storage (LCCOS) and levelized cost of energy (LCOE) metrics, J. Energy Storage 29 (2020) 101345, https://doi.org/10.1016/j.est.2020.101345.
[80] V. Jülch, Comparison of electricity storage options using levelized cost of storage (LCOS) method, Appl. Energy 183 (2016) 1594–1606, https://doi.org/10.1016/j.apenergy.2016.08.165.
[81] C.S. Lai, M.D. McCulloch, Levelized cost of electricity for solar photovoltaic and electrical energy storage, Appl. Energy 190 (2017) 191–203, https://doi.org/10.1016/j.apenergy.2016.12.153.
[82] M.M. Rahman, A.O. Oni, E. Gemechu, A. Kumar, Assessment of energy storage technologies: A review, Energy Convers. Manag. 223 (2020) 113295, https://doi.org/10.1016/j.enconman.2020.113295.
[83] K. Scott, S. Hendrickson, N. Ryan, A. Dawson, K. Kort, J. Capotosto, B. Shrager, V. Siberry, P. Spitsen, S. Babinec, P. Balducci, Z. Zhou, D. Crane, K. Cummins, M. Klembara, V. Chan, L. Tian, J. Shah, J. Wagner, Pathways to Commercial Liftoff: Long Duration Energy Storage, DOE, Office of Technology Transitions, March 2023 https://liftoff.energy.gov/long-duration-energy-storage/.
[84] P.C. Nikolaos, F. Marios, K. Dimitris, A review of pumped hydro storage systems, Energies 16 (11) (2023) 4516, https://doi.org/10.3390/en16114516.
[85] J.W. Saulsbury, A comparison of the environmental effects of open-loop and closed-loop pumped Storage hydropower, in: DOE, 2020, https://doi.org/10.2172/1616475.
[86] Great Lakes Fishery Trust (GLFT), About the Trust (accessed 2025), https://www.glft.org/about.
[87] S. Karambelkar, A. Cantor, T.-K. Bui, B. Turley, M. Fischer, S. Ames, Pumped Storage hydropower in the United States: Emerging importance, environmental and social impacts, and critical considerations, WIREs Water. 12 (3) (2025) e70017, https://doi.org/10.1002/wat2.70017.
[88] U.S. Nuclear Regulatory Commission (NRC), *Palisades Nuclear Plant*, (accessed 2025) https://www.nrc.gov/info-finder/reactors/pali.html.
[89] M. Ak, E. Kentel, S. Kucukali, A fuzzy logic tool to evaluate low-head hydropower Technologies at the Outlet of wastewater treatment plants, Renew. Sust. Energ. Rev. 68, Part 1 (2017) 727–737, https://doi.org/10.1016/j.rser.2016.10.010.
[90] J. Malewitz, Michigan's UP is full of closed mines, in: Technology may give them new life, Michigan Environment Watch, 2019. https://www.bridgemi.com/michigan-environment-watch/michigans-full-closed-mines-technology-may-give-them-new-life.
[91] R. Sidortsov, S. Tiwari, T. Scarlett, A. Dyreson, D. Watkins, PUSHing for storage: A case for repurposing decommissioned mines for pumped underground storage hydro (PUSH) in the United States, 2021. Technical Report.
[92] Center for Climate and Energy Solutions (C2ES), getting to zero: A U.S. climate Agenda, C2ES. (2020) https://www.c2es.org/getting-to-zero-a-u-s-climate-agenda-report/#:~:text=Getting%20to%20Zero%3A%20A%20U.S.%20Climate%20Agenda%20recommends%20that%20a,technological%20solutions%2C%20promoting%20cost%2Deffective.
[93] United States of America, The Long-Term Strategy of the United States: Pathways to Net-Zero Greenhouse Gas Emissions by 2050 (Accessible version), United Nations Climate Change. (2021) https://unfccc.int/documents/308100.

[94] Newburger, Emma, Biden Pledges to Slash Greenhouse Gas Emissions in Half by 2030, *CNBC.* (2021) https://www.cnbc.com/2021/04/22/biden-pledges-to-slash-greenhouse-gas-emissions-in-half-by-2030.html.

[95] U.S. EPA (Environmental Protection Agency), Inventory of U.S. greenhouse gas emissions and sinks: 1990–2022 (EPA 430-R-24-004). https://www.epa.gov/ghgemissions/inventory-us-greenhouse-gas-emissions-and-sinks-1990-2022, 2024.

[96] Reuters, Emissions set to rise with global power demand - IEA, *Reuters.* (2022) https://www.reuters.com/business/energy/emissions-set-rise-with-global-power-demand-iea-2022-01-14/#:~:text=Global%20electricity%20demand%20rose%20by,report%20on%20the%20electricity%20sector.

[97] IEA, in: IEA (Ed.), Global Energy Review 2021, 2021. https://www.iea.org/reports/global-energy-review-2021.

[98] E.K. Hart, E.D. Stoutenburg, M.Z. Jacobson, The potential of intermittent renewables to meet electric power demand: Current methods and emerging analytical techniques, Proc. IEEE 100 (2) (2012) 322–334, https://doi.org/10.1109/JPROC.2011.2144951.

[99] M. Esteban, J. Portugal-Pereira, B.C. McLellan, J. Bricker, H. Farzaneh, N. Djalilova, K.N. Ishihara, H. Takagi, V. Roeber, 100% renewable energy system in Japan: Smoothing and ancillary services, Appl. Energy 224 (2018) 698–707, https://doi.org/10.1016/j.apenergy.2018.04.067.

[100] U.S. Department of Energy, Office of Energy Efficiency and Renewable Energy, U. S. Hydropower Market Report 2023 Edition. https://www.energy.gov/eere/water/hydropower-market-reports, 2023.

[101] L. Bird, D. Lew, M. Milligan, E.M. Carlini, A. Estanqueiro, D. Flynn, E. Gomez-Lazaro, H. Holttinen, N. Menemenlis, A. Orths, P.B. Eriksen, J.C. Smith, L. Soder, P. Sorensen, A. Altiparmakis, Y. Yasuda, J. Miller, Wind and solar energy curtailment: A review of international experience, Renew. Sust. Energ. Rev. 65 (2016) 577–586, https://doi.org/10.1016/j.rser.2016.06.082.

[102] A.R. Dehghani-Sanij, E. Tharumalingam, M.B. Dusseault, R. Fraser, Study of energy Storage systems and environmental challenges of batteries, Renew. Sust. Energ. Rev. 104 (2019) 192–208, https://doi.org/10.1016/j.rser.2019.01.023.

[103] P. Devine-Wright, Beyond NIMBYism: Towards an integrated framework for understanding public perceptions of wind energy, Wind Energy. 8 (2005) 125–139, https://doi.org/10.1002/we.124.

[104] Esri, Great Lakes Shorelines, 2017. https://www.arcgis.com/home/item.html?id=d87347457bc84e5c985db9e904b66b10.

[105] National Park Service (NPS), Hydropower Assistance, (accessed 2024). https://www.nps.gov/orgs/1988/index.htm.

[106] C.H. Oglesby, R.G. Hicks, Highway engineering, John Wiley & Sons, N. Y., 1982.

[107] N. Haregeweyn, J. Poesen, J. Nyssen, J. De Wit, M. Haile, G. Govers, S. Deckers, Reservoirs in Tigray (northern Ethiopia): Characteristics and sediment deposition problems, Land Degrad. Dev. 17 (2006) 211–230, https://doi.org/10.1002/ldr.698.

[108] Roberts, N., and Lambert, R., Degradation of Dambo Soils and Peasant Agriculture in Zimbabwe, in Boardman, J., Foster, I.D.L., and Dearing, J.A. (Eds.), *Soil Erosion on Agricultural Land: Proceedings of a Workshop Sponsored by the British Geomorphological Research Group, Coventry, UK,* January 1989. (1990) 537–558, ISBN: 0–417–92602-7, John Wiley & Sons Ltd., Chichester, UK.

[109] J.P. Fitzgerald, E.A. Cooper, F.P. Solomon, Operation of Seneca pumped storage plant, IEEE Trans. Power Appar. Syst. PAS-92 (5) (1973) 1510–1516, https://doi.org/10.1109/TPAS.1973.293695.

[110] E. Comninellis, Ludington pumped Storage project, Journal of the Power Division. 99 (1973) 1, https://doi.org/10.1061/JPWEAM.0000749.

[111] S. Borenstein, J. Bushnell, S. Stoft, The competitive effects of transmission capacity in a deregulated electricity industry, RAND J. Econ. 31 (2) (2000) 294–325, https://doi.org/10.2307/2601042.

[112] R. Kumar, S.K. Singal, Penstock material selection in small hydropower plants using MADM methods, Renew. Sust. Energ. Rev. 52 (2015) 240–255, https://doi.org/10.1016/j.rser.2015.07.018.

[113] O. Schmidt, S. Melchior, A. Hawkes, I. Staffell, Projecting the future Levelized cost of electricity Storage technologies, Joule 3 (2019) 81–100, https://doi.org/10.1016/j.joule.2018.12.008.

[114] A. Berrada, A. Emrani, A. Ameur, Life-cycle assessment of gravity energy storage systems for large-scale application, J. Energy Storage 40 (2021) 102825, https://doi.org/10.1016/j.est.2021.102825.

[115] B. Zakeri, S. Syri, Electrical energy storage systems: A comparative life cycle cost analysis, Renew. Sust. Energ. Rev. 42 (2015) 569–596, https://doi.org/10.1016/j.rser.2014.10.011.

[116] Chen, H. H., *Pumped-Storage Planning and Evaluation Guide,* American Society of Civil Engineers, 1991. Presented at waterpower '91, Denver, CO, July 24–26, 1991. ISBN: 0-87262-814-0.

[117] K. Mongird, V. Viswanathan, J. Alam, C. Vartanian, V. Sprenkle, R. Baxter, Grid Energy Storage Technology Cost and Performance Assessment, Pacific Northwest National Laboratory (2020). DOE/PA-0204, December 2020, https://www.pnnl.gov/sites/default/files/media/file/Final%20-%20ESGC%20Cost%20Performance%20Report%2012-11-2020.pdf.